Electronic Supplementary Information

The challenge with high permittivity acceptors in organic solar cells: A case study with Y series derivatives

Peter Fürk,[a] Suman Mallick,[a] Thomas Rath,*[a,b] Matiss Reinfelds,[a] Mingjian Wu,[c] Erdmann Spiecker,[c] Nikola Simic,[d] Georg Haberfehlner,[d] Gerald Kothleitner,[d] Barbara Ressel,[e] Sarah Holler,[a] Jana B. Schaubeder,[f] Philipp Materna,[g] Heinz Amenitsch,[g] Gregor Trimmel*[a]

[a] Institute for Chemistry and Technology of Materials (ICTM), NAWI Graz, Graz University of Technology, Stremayrgasse 9, 8010 Graz, Austria

[b] Joanneum Research, MATERIALS-Institute for Sensors, Photonics and Manufacturing Technologies, Franz-Pichler Straße 30, 8160 Weiz, Austria

[c] Institute of Micro- and Nanostructure Research & Center for Nanoanalysis and Electron Microscopy (CENEM), Friedrich-Alexander-Universität Erlangen-Nürnberg, Cauerstraße 3, 91058 Erlangen, Germany

[d] Institute of Electron Microscopy and Nanoanalysis, Graz University of Technology, Steyrergasse 17, 8010 Graz, Austria

[e] Laboratory of Quantum Optics, University of Nova Gorica, Vipavska Cesta 11c, 5270 Ajdovščina, Slovenia

[f] Institute of Bioproducts and Paper Technology (BPTI), Graz University of Technology, Inffeldgasse 23, 8010 Graz, Austria

[g] Institute of Inorganic Chemistry, NAWI Graz, Graz University of Technology, Stremayrgasse 9, 8010 Graz, Austria

* Thomas Rath, E-Mail: thomas.rath@tugraz.at

* Gregor Trimmel, E-Mail: gregor.trimmel@tugraz.at

CONTENTS

Methods

Column chromatography was performed using a Biotage "Selekt" automated flash chromatography system with purchased pre-filled columns "Sfär" from Biotage (spherical or irregular silica with particle size from 20 – 60 μm).

NMR spectra were recorded using a Bruker Avance III 300 MHz, a Varian Inova (400 MHz and 500 MHz), and a Jeol ECZR 400 MHz spectrometer. The spectra were processed with the software Jason (Jeol). All deuterated solvents were purchased from EurisoTop GmbH. The spectra were referenced to the TMS (default) or solvent signal.

Mass spectra were measured using a Micromass TofSpec 2E time-of-flight mass spectrometer from Waters and the appropriate software MassLynx Software V3.5 from Micromass/Waters. Matrices were dithranol or DCTB (*trans*-2-[3-(4-tertbutylphenyl)-2methyl2-propenylidene]-malononitrile). All spectra were calibrated with polyethylene glycol as external standard. Atmospheric pressure chemical ionization (APCI) mass spectra were recorded on an Advion ExpressionL CMS mass spectrometer with nitrogen as carrier gas and the included software Advion Mass Express. The samples were applied in solution onto a glass carrier and then directly inserted into the ionization chamber.

Thermogravimetric analysis (TGA) measurements were done on a TGA8000 from Perkin Elmer in aluminium crucibles under helium atmosphere. The used scan range was from 30 to 550 °C with a scan rate of 10 °C min^{-1}.

UV-Vis spectra were recorded on a Shimadzu UV-1800 spectrometer, for both solution (0.01 mg ml^{-1} in chloroform, in 1 cm optical glass cuvettes from Hellma) and thin film (drop cast from 10 mg ml^{-1} chloroform solution) measurements.

Fluorescence spectra were measured on a FluoroLog 3 spectrofluorometer from Horiba Scientific Jobi Yvon together with a R2658 photomultiplier from Hamamtsu. The spectra were measured in solution (approx. 0.01 mg ml^{-1} in chloroform) from 680 − 1050 nm with at an excitation wavelength at 670 nm.

Cyclic voltammetry (CV) was done on a SP-50 single channel potentiostat from BioLogic and the corresponding software EC-Lab® (V11.31). Measurements were done in a three-electrode setup with a Pt disc working electrode (diameter 2 mm), a Pt wire counter electrode (diameter 0.5 mm) and a non-aqueous $Ag/AgNO_3$ reference electrode (0.5 mm Ag wire in a 0.1 M $AgNO_3$ solution in MeCN), with a 0.1 M tetrabutylammonium hexafluorophosphate ($TBAPF_6$) solution in acetonitrile as electrolyte. The respective material was drop coated onto the working electrode in a nitrogen filled glove box. To avoid interference from trapped charges, oxidation and reduction were measured separately with freshly prepared films and a scan speed of 50 mV s^{-1}. Fc/Fc^+ was used as external standard. The orbital energies were calculated using

$$E_{\mathrm{HOMO}} = -\left(E^{\mathrm{ox}}_{\mathrm{onset\,vs.Fc/Fc^+}} + 5.39\right)\,\mathrm{eV}$$

$$\mathrm{E_{LUMO}} = -\left(\mathrm{E^{red}_{onset\,vs.Fc/Fc^+}} + 5.39\right)\,\mathrm{eV}$$

The Fermi energy level of NHE vs. vacuum was taken as 4.75 eV, whereas the redox potential of Fc/Fc^+ vs. NHE was taken as 0.64 V. [1,2]

Ultraviolet photoelectron spectroscopy (UPS) measurements were performed at the CITIUS facility of the Laboratory of Quantum Optics using an R3000 electrons' spectrometer from VG-Scienta.[3] The photon energy was set on the 21st harmonic of the fundamental laser wavelength, that corresponds to 31.5 eV. The photon energy was calibrated on the Fermi level of a clean Cu(110) crystal, in this way it was also possible to determine the binding energies. The overall energy resolution of the system is about 130 meV and the measurements have been performed at room temperature. The HOMO was determined from the emission onset of the UPS spectrum. To evaluate the final energy position, 4.56 eV (work function Cu(110))[4] were added to the value of the emission onset.

Surface free energy (SFE) measurements were done on a Drop Shape Analysis System DSA100 from Krüss GmbH. The system is equipped with an IDS uEye UI306xCP-M video camera (IDS Imaging Development Systems GmbH). The used software was the Krüss Advance v1.8.0.4. The measurements were done with static contact angle measurement method using MilliQ water (H_2O) and diiodomethane (DIM) with a drop size of 2 µl and dispense rate of 2.67 µl s^{-1}. SFEs were the calculated using the Owens-Wendt-Rabel-Kaelble (OWRK)[5] and Wu[6] methods. The Flory Huggins interaction parameter χ was calculated using

$$\chi_{A-B} = \left(\sqrt{A} - \sqrt{B}\right)^2$$

from the SFE values of the two respective components.

Grazing-incidence wide-angle X-ray scattering (GIWAXS) measurements were done on an Anton Paar SAXSpoint 2.0 with a 50 W Cu-K_α X-ray source focused to a 1 mm^2 point source and a Dectrius 2D detector at a sample distance of 140 mm and a grazing angle of 2.0°. The spectra were averaged from six 5 min measurements in a vacuum chamber at 1 mbar, respectively. The films were drop-coated onto silicon substrates (grade: prime, thickness: 625 ± 20 µm) from Siegert Wafer and annealed at 100 °C for 10 min.

Atomic force microscopy (AFM) images were acquired on a Tosca™ 400 atomic force microscope from Anton Paar, using silicon cantilevers (AP-ARROW-NCR from NanoWorld AG) in tapping mode (resonance frequency 285 kHz, force constant 42 N m^{-1}).

TEM investigations – For the electron microscopic analyses, thin films were spin coated onto sodium chloride crystal substrates (Korth Kristalle GmbH). For the transfer to the TEM grid, the sodium chloride crystals were dissolved in deionized water and the resulting floating films were washed several times before they were placed on the TEM grid. The TEM studies were performed using a double Cs-corrected Thermo Fischer Scientific (TFS) Titan Themis 300 microscope at a primary beam energy of 300 keV. This instrument is equipped with a Gatan Image Filter (GIF) Quantum ERS for high-speed STEM-EELS (electron energy-loss spectroscopy) studies as well as energy filtering. The energy filtered selected area electron diffraction (EF-SAED) patterns were acquired in TEM mode using a parallel beam illumination, an area selection aperture including 3.5 µm area of interest, and an energy selecting slit of 10 eV around the zero loss. Energy filtering enhances the contrast of Bragg peaks at small angles by reducing the intense background from inelastic scattering at these angles. The diffraction data were acquired at dose rate of 0.2 – 0.5 $e^-/Å^2s$ and total dose less than 1 $e^-/Å^2$, far less than typical dose budget of radiation damage of these samples. The latter has been systematically evaluated under similar experimental conditions for another BHJ

system (DRCN5T:$PC_{71}BM$) with small molecule donor to be around 5 $e^-/Å^2$ for the π-stacking bonds and more than 30 $e^-/Å^2$ for lamella stacking.[7] The elemental maps were evaluated and quantified using model-based fitting procedure as implemented in Gatan Microscopy Suite software. The S/N STEM-EELS spectrum images (SIs) were acquired on a probe-corrected FEI Titan^3 60−300 microscope equipped with a Gatan Imaging Filter (GIF) Quantum and a Gatan K2 direct electron detection camera. The beam current was ∼100 pA, the beam convergence angle was 19.6 mrad, and the collection angle was 24.2 mrad. The size of the SIs was ∼230 × 230 pixels at a pixel size of 2 nm with a pixel dwell time of 20 ms. The used dispersion was 0.25 eV/ch, leading to a spectral range from 120 eV to ∼1050 eV for the ∼3700 spectral channels of the detector. All spectrum images were treated with principal components analysis (PCA), which allows efficient removal of the Poissonian noise. After PCA treatment, ionization edges of N (K-edge) and S (L-edge) are extracted. To normalize for thickness effects stemming from the inhomogeneity of the polymer film, the ratio of the elemental maps is calculated and displayed.

Permittivity determination of the pristine materials was done by impedance spectroscopy of fabricated parallel-plate capacitors. For the capacitors, devices were built with the setup glass/ITO/PEDOT:PSS/sample/Ag, using the identical methods as for the solar cell fabrication. The PEDOT:PSS layer was used as smoothing layer to obtain homogeneous material layers on top. The sample material was spin-coated from chloroform solutions. With the geometric device parameters, the relative permittivity of the materials was calculated by

$$\varepsilon_{\mathrm{r}} = \frac{Cd}{\varepsilon_0 A}$$

where C is the measured capacitance (as a function of the frequency of the applied electric field), d and A the thickness and area of the acceptor layer, respectively, and ε_0 the permittivity of the vacuum (8.8542×10^{12} F m^{-1}). The layer thicknesses were measured by profilometry. To obtain representative values, 20 - 30 measurements were averaged for each material. The impedance measurements were done on an Alpha-A High-Performance Frequency Analyzer from NOVOCONTROL Technologies with the software WinDETA V6.02. The AC voltage was set to 20 mV (root mean square), the frequency window from 10^2 to 10^6 Hz. All measurements were performed in an Argon glove box at room temperature in dark conditions.

***J-V* curves** were recorded using a Keithley 2400 source meter connected to a LabView-based software. All measurements were done inside a nitrogen glove box. As light source, a Dedolight DLH400 lamp with a similar emission spectrum to AM1.5G was used at an intensity of 100 mW cm^{-2} (calibrated with a monocrystalline silicon WPVS reference solar cell from Fraunhofer ISE). The illumination area was defined with a shadow mask to be 2.65 × 2.65 mm^2. Scans were done from 1.50 V to -0.50 V (step width -0.02 V).

For the **light intensity dependent** measurements, various light filters were inserted between light source and solar cell. The filters were unmounted 25 mm absorptive neutral density filters from Thorlabs Inc. in various filter strengths (transmission values of 0.05, 0.11, 0.74, 4.88, 10.43, 27.60, 31.82, 52.97 and 81.20%, respectively).

For the J_{ph}-V_{eff} **plot**, *JV* curves were recorded from +3 V to -3 V under illuminated and dark conditions. For processing, we followed a literature-known procedure.[8] The photocurrent J_{ph} is defined as the difference of the current density under illuminated (AM1.5G) conditions (J_{light})

and under dark conditions (J_{dark}) ($J_{ph} = J_{light} - J_{dark}$). The effective voltage V_{eff} is defined as the voltage where $J_{ph} = 0$ (V_0) subtracted by the applied voltage (V_{appl}) ($V_{eff} = V_0 - V_{appl}$). From that plot, the exciton dissociation efficiency (η_{diss}) is calculated as the ratio of J_{ph} at short-circuit conditions to J_{ph} at $V_{eff} = 2.0$ V. Similarly, the charge collection efficiency (η_{cc}) is calculated as the ratio of J_{ph} at maximum-power-point conditions to J_{ph} at $V_{eff} = 2.0$ V.

External quantum efficiency (EQE) spectra were measured with a Keithley 2400 source meter connected to a LabView-based software. Light source was a 75 W xenon lamp connected to a Multimode 4-AT monochromator from Amko. During measurement, the incident light beam was chopped at a frequency of 30 Hz. The setup calibration was done using a silicon photodiode (818-UV/DB, Newport Corporation). All spectra were recorded from 380 to 1000 nm with a 10 nm step width.

Profilometry measurements were done on a Bruker DektakXT stylus surface profiling system and a Vision 64 software (Bruker). The line scans were recorded with a 12.5 µm radius stylus tip, over a length of 1000 µm, with a stylus force of 3 mg and resolution of 0.33 µm pt^{-1}.

Solar Cell Fabrication

Pre-patterned glass/ITO substrates (15 × 15 × 1.1 mm^3, 15 Ω sq^{-1}) were cleaned by wiping them with acetone using Kimwipes (Kimberly-Clark), then by sonication in a 2-propanol bath (40 °C, 40 min), followed by blow-drying in a nitrogen stream and finally oxygen plasma etching (99 W, 3 min, FEMTO, Diener Electronics).

For the conventional setup (ITO/PEDOT:PSS/(PM6 or PBDB-T):acceptor/PNDIT-F3N-Br/Ag), a suspension of PEDOT:PSS in water was filtered through a 0.45 µm PTFE syringe filter, then spin-coated (50 µl with 3500 rpm and 1500 rpm s^{-1} for 30 s) onto freshly plasma-etched glass/ITO substrates, followed by thermal annealing at 150 °C for 15 min in ambient conditions. This gave an average film thickness of 30 nm. For the active layer, precursor solutions were prepared by dissolving PM6 or PBDB-T and the respective acceptor in chloroform + 0.5 vol.% 1-chloronaphthalene, in a D/A ratio of 1/1.2 and a total concentration of 14 mg ml^{-1}. The solutions were stirred overnight at RT before deposition. The active layers were applied with varying spin coating parameters (1000 - 5000 rpm), followed by thermal annealing at 100 °C for 10 min. The PNDIT-F3N-Br layer was spincoated from a 0.5 mg ml^{-1} methanol solution with 2000 rpm, 1500 rpm s^{-1} for 30 s. Lastly, an Ag electrode (100 nm, 0.1 – 2.0 Å s^{-1}) layer was applied by thermal evaporation at high vacuum (< 1 × 10^{-5} mbar, thickness monitor: Inficon SQM-160 rate/thickness monitor) through a shadow mask (3 × 3 mm^2).

Synthesis

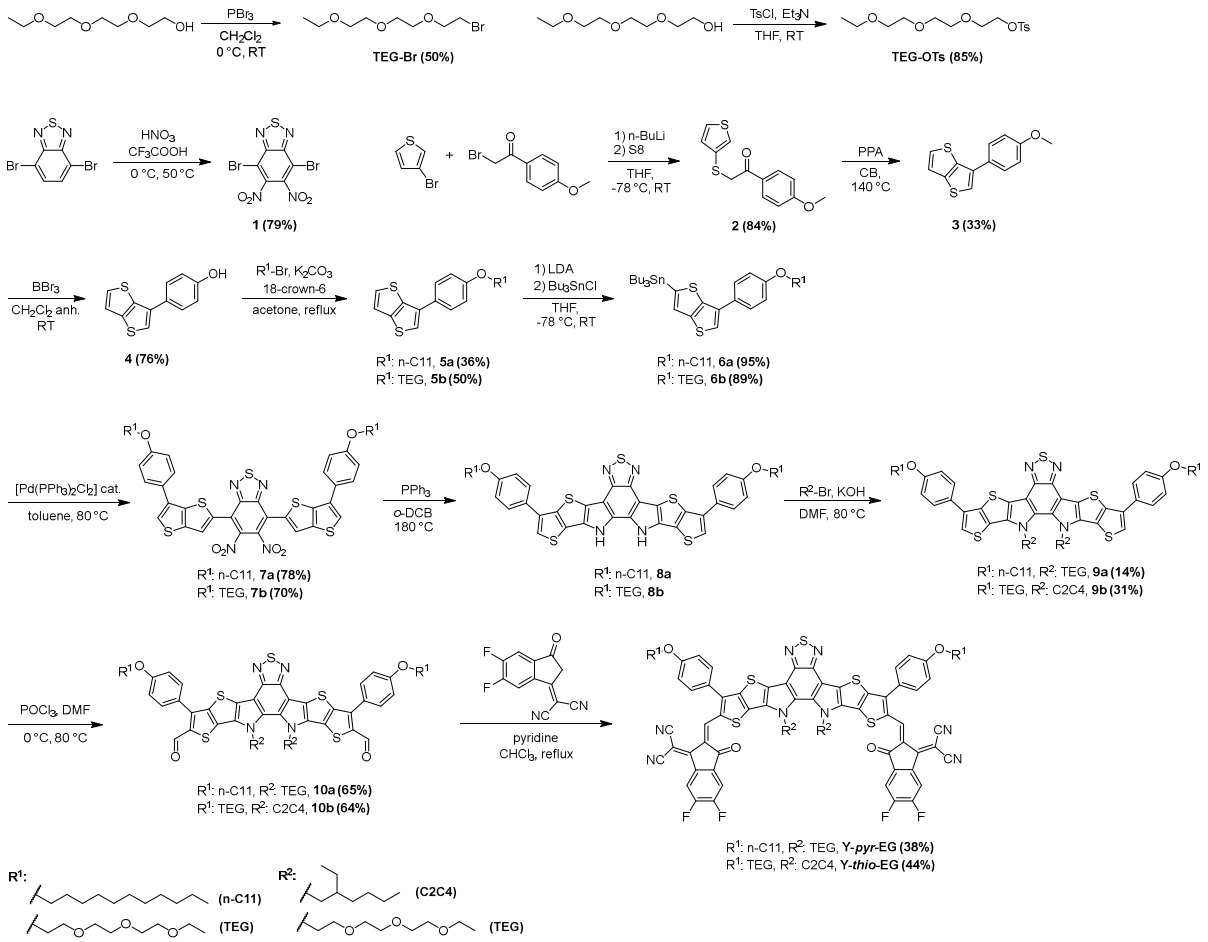

Scheme S1 Full synthesis route for the novel acceptors Y-*thio*-EG and Y-*pyr*-EG.

General

All starting materials were purchased from commercially available sources and used without further purification, unless otherwise stated. The solar cell materials (PM6, PBDB-T, PNDIT-F3N-Br) were purchased from 1-Material. PEDOT:PSS was purchased from Heraeus (CLEVIOS™ P VP AI 4083). Compounds **1**,[9] **2**,[10] **3**,[10] and **TEG-OTs**[11] were prepared according to literature procedures.

*Compound **TEG-Br***

The procedure was adapted from literature.[12] A flame-dried flask under nitrogen atmosphere was charged with 2-(2-(2-ethoxyethoxy)ethoxy)ethan-1-ol (9.00 ml, 51.8 mmol) and 30 ml dry CH_2Cl_2. At 0 °C, PBr_3 (1.97 ml, 20.7 mmol, 1.15 equiv.) was added dropwise over 1 h. The mixture was then stirred at 0 °C for 1 h, and at RT overnight. For workup, the reaction mixture was diluted with 100 ml CH_2Cl_2 and washed with water (2x), brine (1x) and dried with Na_2SO_4. The solvent was removed *in vacuo*. The crude product was purified by dry-flash column chromatography (cyclohexane/ethyl acetate 4/1 to 1/1 *v/v*) to yield the product **TEG-Br** (6.67 g, 50%) as colourless oil.

^{1}H NMR (300 MHz, $CDCl_3$, TMS) δ (ppm): 3.82 (t, J = 6.3 Hz, 2 H), 3.74 – 3.40 (m, 12 H), 1.21 (t, J = 7.0 Hz, 3 H). ^{13}C NMR (75 MHz, $CDCl_3$, TMS) δ (ppm): 71.16, 70.70, 70.57, 70.50, 69.78, 66.56, 30.29, 15.14.

*Compound **4***

The procedure was adapted from literature.[13] A flame-dried Schlenk tube under nitrogen atmosphere was charged with dry compound **3** (4.682 g, 19.01 mmol, 1 equiv.) and 20 ml dry CH_2Cl_2. The solution was cooled to 0 °C and 1 M BBr_3 in CH_2Cl_2 (19.0 ml, 19.01 mmol, 3 equiv.) was added dropwise, which led to immediate red colourization. The solution was stirred for 15 min at 0 °C, then at RT overnight. When TLC control indicated full conversion, the reaction was diluted with 100 ml CH_2Cl_2 and quenched by adding 100 ml water. 10 wt.% KOH was added until a pH of approx. 9-10 was reached and the solution was stirred for 15 min. The solution was then acidified with 3 M HCl to a pH of approx. 2, and the mixture was extracted with CH_2Cl_2 (3 × 40 ml). The combined organic phase was dried with Na_2SO_4, and the solvent removed *in vacuo*. The crude oil was purified by a short silica plug (eluent cyclohexane/ethyl acetate 1/1 *v*/*v*) to give the product **4** (3.343 g, 76%) as a colourless oil.

^{1}H NMR (500 MHz, $(CD_3)_2SO$, TMS) δ (ppm): 9.67 (s, 1 H), 7.79 (d, J = 1.5 Hz, 1 H), 7.74 (dd, J = 5.2, 1.5 Hz, 1 H), 7.62 (d, J = 8.7 Hz, 2 H), 7.51 (d, J = 5.2 Hz, 1 H), 6.90 (d, J = 8.7 Hz, 2 H). MS (APCI) *m/z* for $C_{12}H_7OS_2^-$ $[M-H]^-$: calcd. 231.0, found 230.8.

*Compound **5a***

A flame-dried flask under nitrogen atmosphere was charged with compound **4** (1.68 g, 7.22 mmol), 1-bromoundecane (5.2 ml, 23mmol), K_2CO_3 (1.50 g, 11 mmol), a spatula tip of 18-crown-6 and 25 ml dry acetone. The mixture was refluxed overnight, which gave an orange reaction mixture. For workup, the reaction mixture was diluted with 200 ml ether and filtered. The filtrate was washed with water (2x), brine, and dried with Na_2SO_4. The solvent was removed *in vacuo*, giving the crude product as dark orange oil. The crude product was purified by recrystallization from hot ethanol, to give the product **5a** (1.02 g, 36%) as colourless solid.

^{1}H NMR (300 MHz, $CDCl_3$, TMS) δ (ppm): 7.68 (d, J = 8.7 Hz, 2 H), 7.43 (d, J = 5.3 Hz, 1 H), 7.39 (s, 1 H), 7.30 (d, J = 5.3 Hz, 1 H), 6.99 (d, J = 8.7 Hz, 2 H), 4.01 (t, J = 6.4 Hz, 2 H), 1.81 (m, 2 H), 1.48 (m, 2 H), 1.40 – 1.21 (m, 14 H), 0.88 (t, J = 7.2 Hz, 3 H). ^{13}C NMR (100 MHz, $CDCl_3$, TMS) δ (ppm): 158.79, 139.46, 137.96, 134.21, 127.51, 127.36, 127.10, 121.08, 119.85, 114.91, 68.14, 31.97, 29.76, 29.68, 29.65, 29.47, 29.40, 29.34, 26.12, 22.75, 14.18. MS (APCI) *m/z* for $C_{23}H_{31}O_7S_2^+$ $[M+H]^+$: calcd. 387.2, found 387.2.

*Compound **5b***

A flame-dried flask under nitrogen atmosphere was charged with compound **4** (1.68 g, 7.22 mmol), the side chain **TEG-Br** (2.94 ml, 12.2 mmol), K_2CO_3 (1.50 g, 11 mmol), a spatula tip of 18-crown-6 and 25 ml dry acetone. The mixture was refluxed overnight. For workup, the reaction mixture was diluted with 200 ml ethyl acetate and washed with water (2x), brine, and dried with Na_2SO_4. The solvent was removed *in vacuo*, and the crude product purified by column chromatography (eluent dichloromethane/ethyl acetate 2% to 15% vol.%) to give the product **5b** (1.42 g, 50%) as colourless liquid.

^{1}H NMR (300 MHz, $CDCl_3$, TMS) δ (ppm): 7.68 (d, J = 8.8 Hz, 2 H), 7.43 (dd, J = 5.3, 1.5 Hz, 1 H), 7.40 (d, J = 1.5 Hz, 1 H), 7.30 (d, J = 5.3 Hz, 1 H), 7.02 (d, J = 8.8 Hz, 2 H), 4.19 (t, J = 4.7 Hz, 2 H), 3.89 (t, J = 5.1 Hz, 2 H), 3.79 – 3.46 (m, 10 H), 1.21 (t, J = 7.0 Hz, 3 H). MS (APCI) *m/z* for $C_{20}H_{25}O_4S_2^+$ $[M+H]^+$: calcd. 393.1, found 393.1.

*Compound **6a***

The procedure was adapted from literature.[14] A flame-dried Schlenk flask under nitrogen atmosphere was charged with dry compound **5a** (0.839 g, 2.17 mmol), followed by 3 vacuum-flush cycles. 50 ml of dry THF were added to give a light orange colour, and the mixture was cooled to -78 °C. At that temperature, 2 M LDA (1.30 ml, 2.60 mmol, 1.2 equiv.) was added dropwise, followed by stirring for 1 h. The reaction mixture turned dark blue. Still at -78 °C, the Bu_3SnCl (0.74 ml, 2.60 mmol, 1.2 equiv.) was added dropwise, which led to immediate decolourization of the solution. After full addition, the flask was let warm to RT and stirred overnight. For workup, the reaction was quenched by adding 25 ml saturated KF solution. The mixture was extracted with cyclohexane (3x) and the combined organic phase washed with brine, dried with Na_2SO_4, and the solvent was removed *in vacuo*. The crude product **6a** (1.48 g) was used for the next step without further purification.

MS (APCI) *m/z* for $C_{35}H_{57}OS_2Sn^+$ $[M+H]^+$: calcd. 677.28, found 677.2.

*Compound **6b***

The procedure was adapted from literature.[14] A flame-dried Schlenk flask under nitrogen atmosphere was charged with dry compound **5b** (1.406 g, 3.58 mmol), followed by 3 vacuum-flush cycles. 50 ml of dry THF were added to give a light brown colour, and the mixture was cooled to -78 °C. At that temperature, 2 M LDA (2.30 ml, 4.45 mmol, 1.2 equiv.) was added dropwise, followed by stirring for 1 h. Still at -78 °C, the Bu_3SnCl (1.20 ml, 4.30 mmol, 1.2 equiv.) was added dropwise. After full addition, the flask was let warm to RT and stirred overnight. For workup, the reaction was quenched by adding 50 ml saturated KF solution. The mixture was extracted with cyclohexane (3x) and the combined organic phase washed with brine, dried with Na_2SO_4, and the solvent was removed *in vacuo*. The crude product **6b** (2.63 g) was used for the next step without further purification.

MS (APCI) *m/z* for $C_{32}H_{51}O_4S_2Sn^+$ $[M+H]^+$: calcd. 683.22, found 683.2.

*Compound **7a***

The procedure was adapted from literature.[14] A flame-dried Schlenk flask under nitrogen atmosphere was charged with dry compound **1** (378 mg, 0.990 mmol), dry crude compound **6a** (1.48 g) and the catalyst $[Pd(PPh_3)_2Cl_2]$ (69 mg, 0.099 mmol). After 3 vacuum-flush cycles, 30 ml dry toluene were added and the mixture was stirred at 80 °C overnight. The reaction mixture turned dark red. For workup, the solvent was removed *in vacuo* and the crude product was purified by column chromatography (eluent cyclohexane/dichloromethane 10% to 30% vol.%), followed by recrystallization by dissolving in 20 ml hot toluene and overlayering with 40 ml MeOH. This gave the product **7a** (373 mg, 38%) as red solid.

^{1}H NMR (300 MHz, $CDCl_3$, TMS) δ (ppm): 7.76 (s, 2 H), 7.68 (d, J = 8.8 Hz, 4 H), 7.55 (s, 2 H), 7.02 (d, J = 8.8 Hz, 4 H), 4.02 (t, J = 6.6 Hz, 4 H), 1.88 – 1.74 (m, 4 H), 1.51 – 1.42 (m, 4 H), 1.42 – 1.18 (m, 28 H), 0.88 (t, J = 7.0 Hz, 6 H). ^{13}C NMR (75 MHz, $CDCl_3$, TMS) δ (ppm): 159.29, 152.29, 142.39, 139.90, 134.67, 134.02, 130.73, 127.83, 126.70, 124.41, 124.05, 121.55, 115.20, 77.35, 68.33, 32.06, 29.77, 29.75, 29.56, 29.49, 29.41, 26.21, 22.84, 14.27.

*Compound **7b***

The procedure was adapted from literature.[14] A flame-dried Schlenk flask under nitrogen atmosphere was charged with dry compound **1** (625 mg, 1.63 mmol), dry crude compound **6b** (2.63 g) and the catalyst [$Pd(PPh_3)_2Cl_2$] (57 mg, 0.081 mmol). After 3 vacuum-flush cycles, 30 ml dry toluene were added and the mixture was stirred at 85 °C overnight. The reaction mixture turned dark red. For workup, the solvent was removed *in vacuo* and the crude product was purified precipitation from hot toluene and cyclohexane to remove aliphatic impurities. This was followed by column chromatography (eluent dichloromethane/acetone 0% to 15% vol.%), to obtain the product **7b** (1.14 g, 70%) as red solid.

^{1}H NMR (300 MHz, $CDCl_3$, TMS) δ (ppm): 7.72 (s, 2 H), 7.64 (d, J = 8.8 Hz, 4 H), 7.52 (s, 2 H), 7.01 (d, J = 8.8 Hz, 4 H), 4.18 (t, J = 5.3 Hz, 4 H), 3.88 (t, J = 5.3 Hz, 4 H), 3.80 – 3.44 (m, 20 H), 1.20 (t, J = 7.2 Hz, 6 H). ^{13}C NMR (75 MHz, $CDCl_3$, TMS) δ (ppm): 158.71, 152.01, 142.10, 141.70, 139.71, 134.34, 130.66, 127.57, 126.83, 124.39, 123.90, 121.22, 115.21, 70.89, 70.74, 70.67, 69.84, 69.71, 67.60, 66.65, 15.20.

*Compound **8a***

A flame-dried flask under nitrogen atmosphere was charged with compound **7a** (708 mg, 0.711 mmol), PPh_3 (2.78 g, 10.7 mmol) and 15 ml of dry *o*-dichlorobenzene. The dark red solution was stirred at 180 °C overnight. For workup, the mixture was cooled to RT, 50 ml MeOH was added and the reaction mixture stirred for 1 h. The supernatant was decanted, leaving a dark orange viscous liquid as crude product. The crude product was dried *in vacuo* and used without further purification for the next step.

*Compound **8b***

A flame-dried flask under nitrogen atmosphere was charged with compound **7b** (1.08 g, 1.07 mmol), PPh_3 (3.93 g, 15.0 mmol) and 25 ml of dry *o*-dichlorobenzene. The dark red solution was stirred at 180 °C overnight. For workup, the mixture was cooled to RT, 50 ml MeOH was added and the reaction mixture stirred for 1 h. The supernatant was decanted, leaving a dark orange viscous liquid as crude product. The crude product was dried *in vacuo* and used without further purification for the next step.

*Compound **9a***

A flame-dried flask under nitrogen atmosphere was charged with all of compound **8a**, K_2CO_3 (590 mg, 4.27 mmol), the alkylating agent **TEG-OTs** (2.10 g, 6.49 mml) and 15 ml dry DMF. The reaction was stirred at 80 °C overnight. For workup, the reaction mixture was diluted with 100 ml dichloromethane and washed with water (5x), brine and dried with Na_2SO_4. The solvent was removed *in vacuo*, and the crude was purified by column chromatography (eluent dichloromethane/ethyl acetate step gradient 0% to 50%). This gave the product **9a** (125 mg, 14%) as orange solid.

^{1}H NMR (300 MHz, $CDCl_3$, TMS) δ (ppm): 7.65 (d, J = 8.9 Hz, 4 H), 7.19 (s, 2 H), 6.90 (d, J = 8.9 Hz, 4 H), 4.87 (t, J = 6.4 Hz, 4 H), 3.93 (t, J = 6.4 Hz, 4 H), 3.81 (t, J = 6.1 Hz, 4 H), 3.39 – 3.08 (m, 20 H), 1.83 – 1.68 (m, 4 H), 1.49 – 1.36 (m, 4 H), 1.36 – 1.12 (m, 28 H), 1.01 (t, J = 7.2 Hz, 6 H), 0.82 (t, J = 6.8 Hz, 6 H). ^{13}C NMR (75 MHz, $CDCl_3$, TMS) δ (ppm): 158.98, 147.37, 139.90, 136.59, 135.92, 131.32, 129.81, 127.99, 127.74, 126.66, 124.05,

122.99, 118.24, 114.89, 111.72, 70.97, 70.55, 70.34, 69.84, 69.59, 68.16, 66.46, 50.49, 31.95, 29.67, 29.64, 29.48, 29.38, 29.33, 26.12, 22.72, 15.09, 14.15.

*Compound **9b***

A flame-dried flask under nitrogen atmosphere was charged with all of compound **8b**, K_2CO_3 (887 mg, 6.42 mmol), the side chain 2-ethylhexyl bromide (1.15 ml, 6.42 mml), a spatula tip of NaI and 15 ml dry DMF. The reaction was stirred at 80 °C overnight. For workup, diluted the reaction mixture with 100 ml dichloromethane and washed with water (5x), brine and dried with Na_2SO_4. The solvent was removed *in vacuo*, and the crude was purified by column chromatography (eluent dichloromethane/ethyl acetate step gradient 0% to 50%). This gave the product **9b** (404 mg, 31%) as orange solid.

^{1}H NMR (300 MHz, $CDCl_3$, TMS) δ (ppm): 7.79 (d, J = 8.8 Hz, 4 H), 7.38 (s, 2 H), 7.04 (d, J = 8.8 Hz, 4 H), 4.68 (d, J = 6.2 Hz, 4 H), 4.19 (t, J = 5.3 Hz, 4 H), 3.89 (t, J = 5.3 Hz, 4 H), 3.80 – 3.48 (m, 20 H), 2.18 – 2.05 (m, 2 H), 1.22 (t, J = 7.2 Hz, 6 H), 1.15 – 1.04 (m, 4 H), 1.04 – 0.86 (m, 12 H), 0.70 – 0.56 (m, 12 H). ^{13}C NMR (75 MHz, $CDCl_3$, TMS) δ (ppm): . 158.67, 147.65, 139.99, 136.84, 135.94, 131.64, 127.87, 127.18, 124.48, 123.04, 118.64, 115.12, 111.53, 70.89, 70.75, 70.68, 69.85, 69.74, 67.58, 66.63, 60.35, 55.06, 40.06, 29.71, 27.75, 22.75, 15.21, 13.74, 10.07.

*Compound **10a***

A flame-dried flask under nitrogen atmosphere was charged with compound **9a** (125 mg, 0.100 mmol) and 10 ml dry DMF. At 0 °C, $POCl_3$ (0.18 ml, 2.0 mmol) was added dropwise, which turned the reaction mixture dark red. After stirring at 0 °C for 1 h, the mixture was stirred at 80 °C overnight. For workup, the reaction was cooled to RT and quenched by adding 50 ml 2 M K_2CO_3 followed by stirring for 15 min. The mixture was then extracted with dichloromethane (3x). The combined orange phase (clear orange solution) was washed with brine (2x), dried with Na_2SO_4, and the solvent removed *in vacuo*. The crude product was purified by column chromatography (eluent dichloromethane/acetone step gradient 0% to 10%) to obtain the product **10a** (84 mg, 65%) as orange solid.

^{1}H NMR (300 MHz, $CDCl_3$, TMS) δ (ppm): 9.85 (s, 2 H), 7.55 (d, J = 8.7 Hz, 4 H), 7.00 (d, J = 8.7 Hz, 4 H), 4.94 (t, J = 5.7 Hz, 4 H), 3.99 (t, J = 6.4 Hz, 4 H), 3.89 (t, J = 5.3 Hz, 4 H), 3.44 – 3.10 (m, 20 H), 1.87 – 1.71 (m, 4 H), 1.52 – 1.38 (m, 4 H), 1.38 – 1.12 (m, 28 H), 1.02 (t, J = 6.8 Hz, 6 H), 0.82 (t, J = 7.2 Hz, 6 H). ^{13}C NMR (100 MHz, $CDCl_3$, TMS) δ (ppm): 184.10, 160.59, 147.20, 142.83, 136.51, 136.50, 132.61, 131.01, 131.01, 128.79, 127.70, 124.04, 115.34, 112.53, 71.04, 70.62, 70.43, 69.94, 69.69, 68.41, 66.61, 50.61, 32.01, 29.73, 29.72, 29.70, 29.52, 29.45, 29.32, 26.17, 22.79, 15.16, 14.22.

*Compound **10b***

A flame-dried flask under nitrogen atmosphere was charged with compound **9b** (404 mg, 0.340 mmol) and 12 ml dry DMF. At 0 °C, $POCl_3$ (0.30 ml, 3.4 mmol) was added dropwise, which turned the reaction mixture dark red. After stirring at 0 °C for 1 h, the mixture was stirred at 80 °C overnight. For workup, the reaction was cooled to RT and quenched by adding 50 ml 2 M K_2CO_3 followed by stirring for 15 min. The mixture was then extracted with dichloromethane (3x). The combined orange phase (clear orange solution) was washed with brine (2x), dried with Na_2SO_4, and the solvent removed *in vacuo*. The crude product was

purified by column chromatography (eluent dichloromethane/acetone step gradient 0% to 10%) to obtain the product **10b** (270 mg, 64%) as orange solid.

^{1}H NMR (300 MHz, $CDCl_3$, TMS) δ (ppm): 9.96 (s, 2 H), 7.72 (d, J = 8.7 Hz, 4 H), 7.15 (d, J = 8.7 Hz, 4 H), 4.71 (d, J = 5.0 Hz, 4 H), 4.27 (t, J = 5.3 Hz, 4 H), 3.95 (t, J = 5.3 Hz, 4 H), 3.85 – 3.46 (m, 20 H), 2.13 – 2.00 (m, 2 H), 1.23 (t, J = 7.0 Hz, 6 H), 1.16 – 0.86 (m, 16 H), 0.77 – 0.56 (m, 12 H).

Compound ***Y*-pyr-*EG***

A round bottom flask was charged with compound **10a** (84 mg, 0.064 mmol) and 2-(5,6-difluoro-3-oxo-2,3-dihydro-1H-inden-1-ylidene)malononitrile (118 mg, 0.514 mmol). The flask was flushed under nitrogen for 10 min, then 10 ml chloroform were added. After full dissolution (amberlike colour), pyridine (0.31 ml, 3.85 mmol) was added, which led to an immediate colour change to dark blue. The mixture was refluxed overnight. For workup, the reaction mixture was cooled to RT, 50 ml of MeOH were added and the mixture stirred for 30 min. Subsequently, the dark blue precipitate was filtered and washed with MeOH. The crude product was purified by column chromatography (eluent chloroform/methanol step gradient 0% to 1.5%, second column with eluent dichloromethane/ethyl acetate 10%), to give the product **Y-*pyr*-EG** (42 mg, 38%) as dark blue solid.

^{1}H NMR (400 MHz, $CDCl_3$, TMS) δ (ppm): 8.71 (s, 2 H), 8.43 (dd, J = 9.9, 6.5 Hz, 2 H), 7.63 (dd, J = 7.7, 7.7 Hz, 2 H), 7.54 (d, J = 8.8 Hz, 4 H), 7.12 (d, J = 8.8 Hz, 4 H), 5.19 (t, J = 5.4 Hz, 4 H), 4.13 – 4.05 (m, 8 H), 3.50 – 3.45 (m, 4 H), 3.35 – 3.28 (m, 8 H), 3.28 – 3.20 (m, 8 H), 1.91 – 1.83 (m, 4 H), 1.56 – 1.48 (m, 4 H), 1.38 – 1.26 (m, 28 H), 1.04 (t, J = 7.0 Hz, 6 H), 0.89 (t, J = 6.8 Hz, 6 H). ^{13}C NMR (100 MHz, $CDCl_3$, TMS) δ (ppm): 185.76, 161.36, 158.34, 152.95, 152.80, 151.84, 147.13, 144.78, 138.40, 137.35, 134.50, 134.27, 134.21, 133.71, 132.75, 131.84, 131.21, 124.28, 120.66, 115.99, 114.79, 114.71, 114.57, 113.69, 113.66, 71.08, 70.62, 70.48, 70.03, 69.67, 69.32, 68.55, 66.59, 51.23, 32.03, 29.78, 29.76, 29.72, 29.56, 29.47, 29.29, 26.16, 22.80, 15.15, 14.23. HR-MS (MALDI-TOF) *m/z* for $C_{94}H_{94}F_4N_8O_{10}S_5^+$ $[M]^+$: calcd. 1730.5632, found 1730.5767. UV-Vis $\lambda_{max}(CHCl_3)$/nm 728 (ε/dm^3 mol^{-1} cm^{-1} 1.61 × 10^5).

Compound ***Y*-thio-*EG***

A round bottom flask was charged with compound **10b** (120 mg, 0.098 mmol) and 2-(5,6-difluoro-3-oxo-2,3-dihydro-1H-inden-1-ylidene)malononitrile (90 mg, 0.39 mmol). The flask was flushed under nitrogen for 10 min, then 10 ml chloroform were added. After full dissolution (amberlike colour), pyridine (0.47 ml, 5.88 mmol) was added, which led to an immediate colour change to dark blue. The mixture was refluxed overnight. For workup, the reaction mixture was cooled to RT, 50 ml of MeOH were added and the mixture stirred for 30 min. Subsequently, the dark blue precipitate was filtered and washed with MeOH. The crude product was purified by column chromatography (eluent chloroform/methanol step gradient 0% to 1.5%), followed by recrystallization from ethyl acetate/cyclohexane to give the product **Y-*thio*-EG** (59 mg, 44%) as dark blue solid.

^{1}H NMR (400 MHz, $CDCl_3$, TMS) δ (ppm): 8.80 (s. 2 H), 8.50 (dd, J = 10.0, 6.5 Hz, 2 H), 7.71 (dd, J = 7.7, 7.7 Hz, 2 H), 7.60 (d, J = 8.8 Hz, 4 H), 7.17 (d, J = 8.8 Hz, 4 H), 4.78 (t, J = 6.1 Hz, 4 H), 4.28 (t, J = 5.0 Hz, 4 H), 3.94 (t, J = 5.2 Hz, 4 H), 3.81 – 3.77 (m, 4 H),

3.75 – 3.67 (m, 8 H), 3.65 – 3.60 (m, 4 H), 3.55 (q, J = 7.0 Hz, 4 H), 2.17 – 2.04 (m, 2 H), 1.26 – 1.16 (m, 10 H), 1.11 – 0.94 (m, 12 H), 0.78 – 0.63 (m, 12 H). ^{13}C NMR (100 MHz, $CDCl_3$, TMS) δ (ppm): 185.98, 160.96, 158.93, 155.72, 153.14, 151.76, 147.54, 144.75, 138.90, 137.76, 134.98, 133.84, 133.16, 131.84, 131.37, 124.95, 121.11, 116.12, 114.71, 113.76, 113.66, 112.71, 112.52, 71.03, 70.86, 70.79, 69.95, 69.67, 69.37, 67.87, 66.75, 55.71, 40.52, 29.80, 27.88, 23.37, 22.92, 15.29, 13.84, 10.15. HR-MS (MALDI-TOF) *m/z* for $C_{88}H_{82}F_4N_8O_{10}S_5^+$ $[M]^+$: calcd. 1646.4694, found 1646.4894. UV-Vis $\lambda_{max}(CHCl_3)$/nm 727 (ε/dm^3 mol^{-1} cm^{-1} 1.58 × 10^5).

Figures & Tables

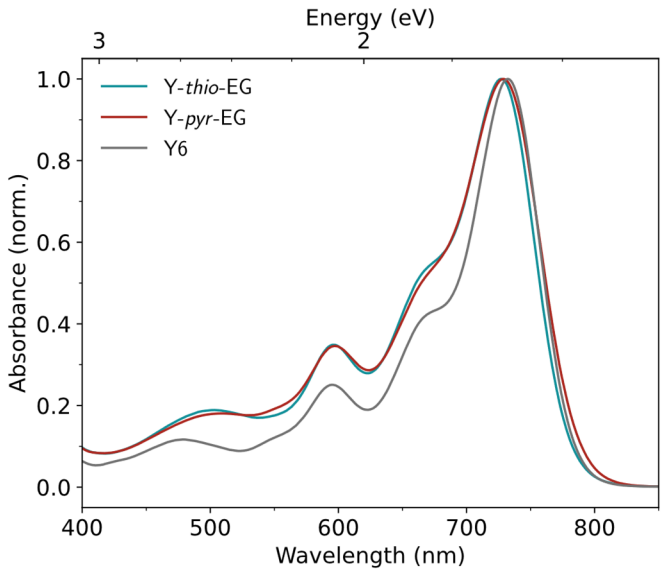

Fig. S1 UV-Vis spectra in chloroform.

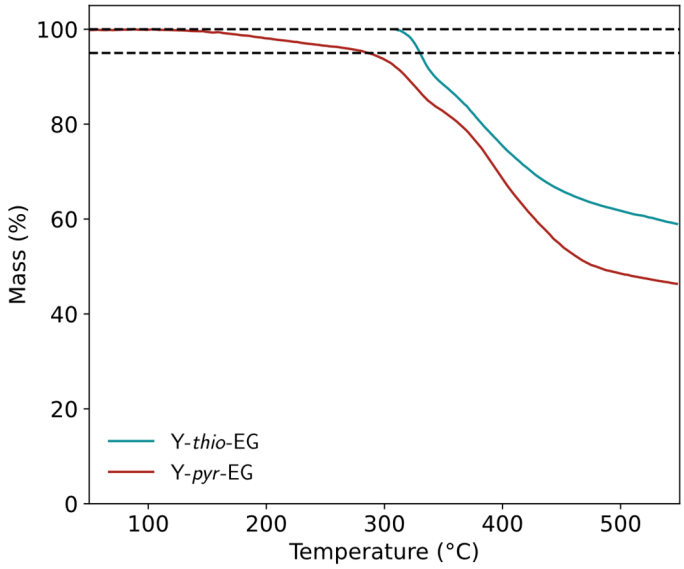

Fig. S2 TGA measurement of new acceptors. Dashed lines indicate 100% and 95% weight.

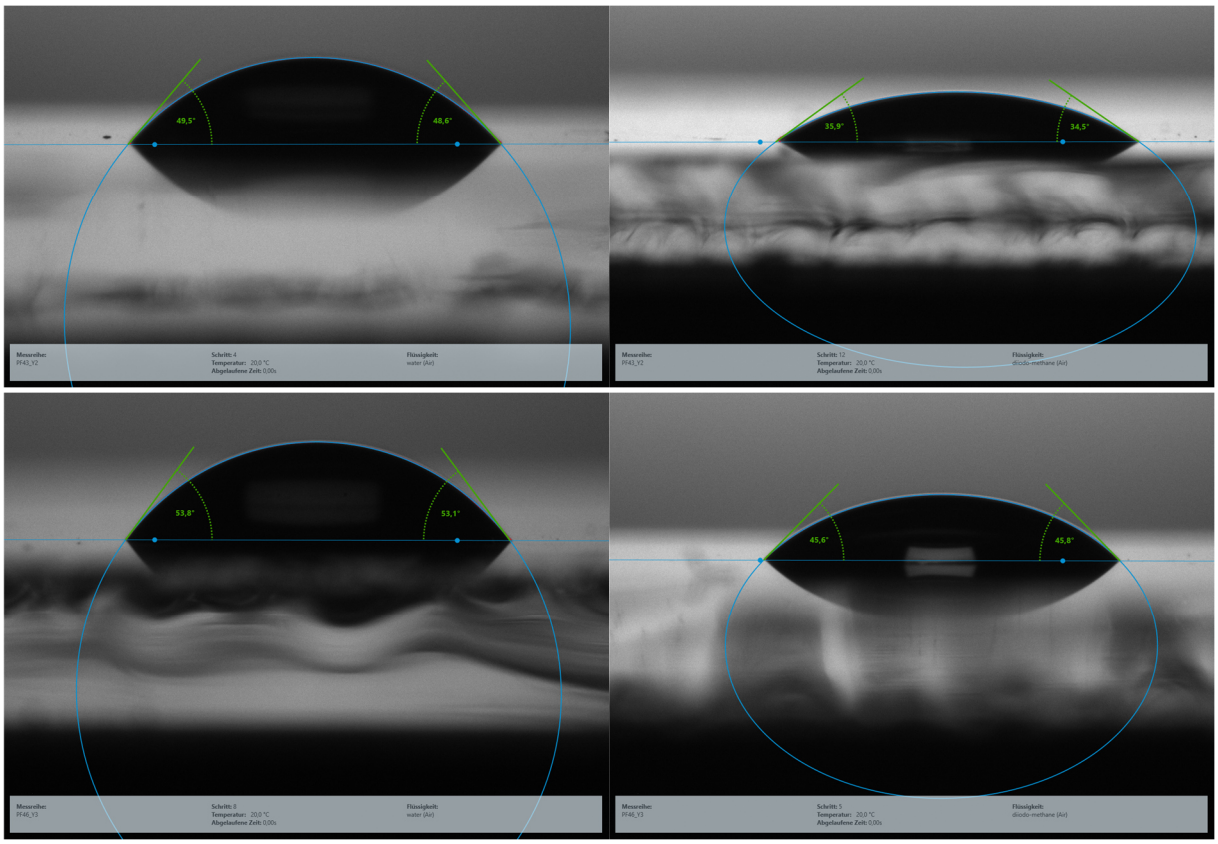

Fig. S3 Contact angle measurements of (top) Y-*thio*-EG and (bottom) Y-*pyr*-EG, with (left) water and (right) diiodomethane drops, respectively.

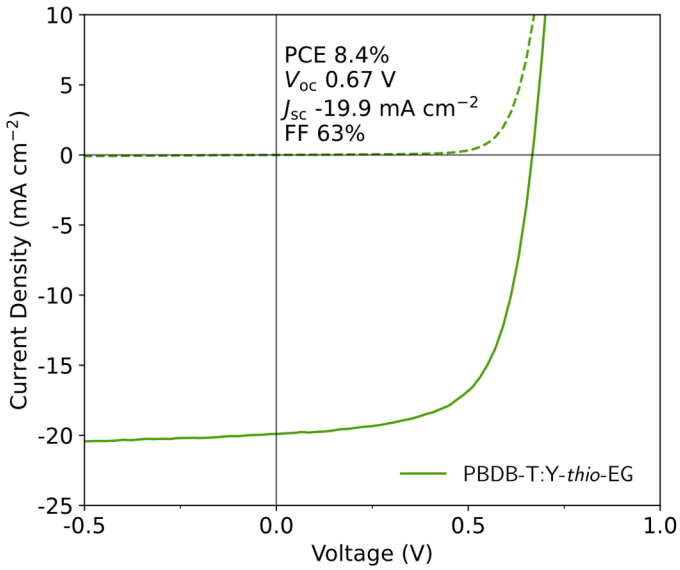

Fig. S4 *JV* curve of PBDB-T:Y-*thio*-EG OSCs (identical setup and preparation as PM6 based OSCs).

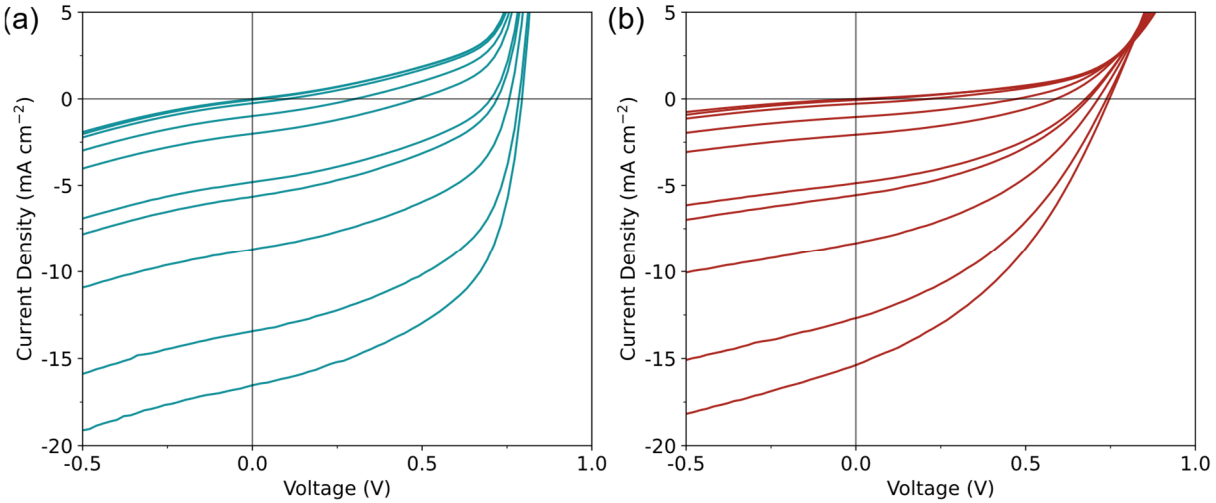

Fig. S5 *JV* curves from light intensity measurements using filters with various transmissions, of (a) Y-*thio*-EG and (b) Y-*pyr*-EG.

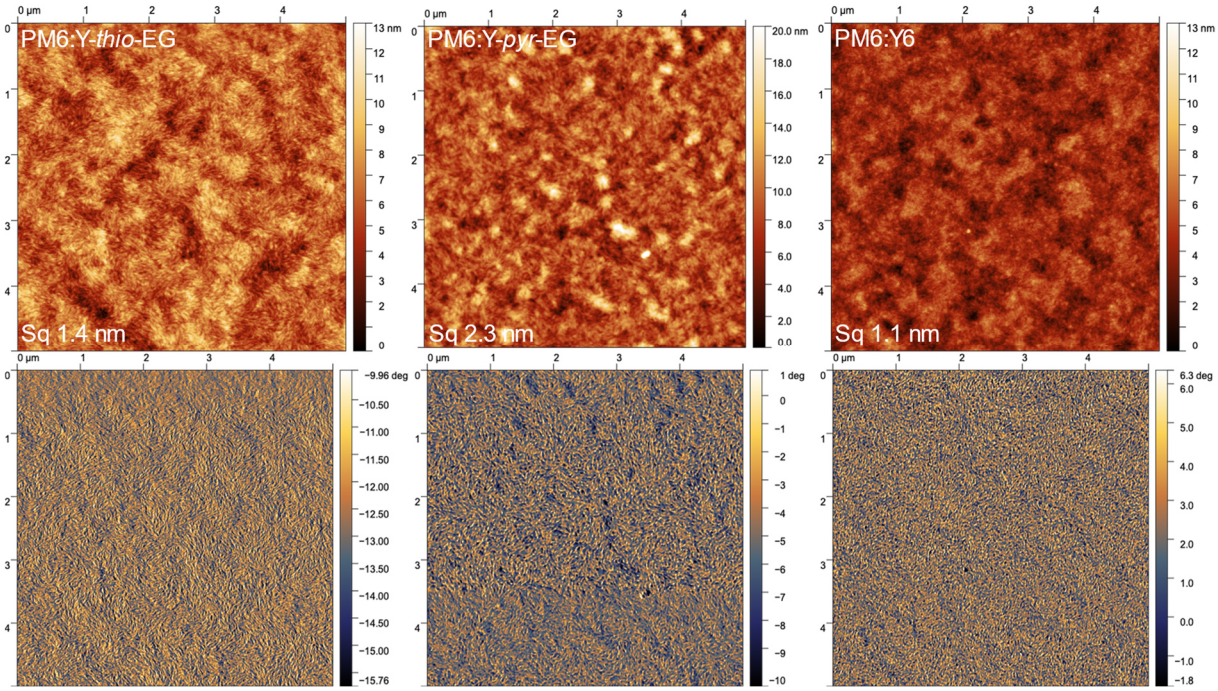

Fig. S6 AFM images (5×5 μm^2) with (top) height and (bottom) phase images of PM6:Y-*thio*-EG, PM6:Y-*pyr*-EG, and PM6:Y6 (films deposited onto ITO/PEDOT:PSS substrates).

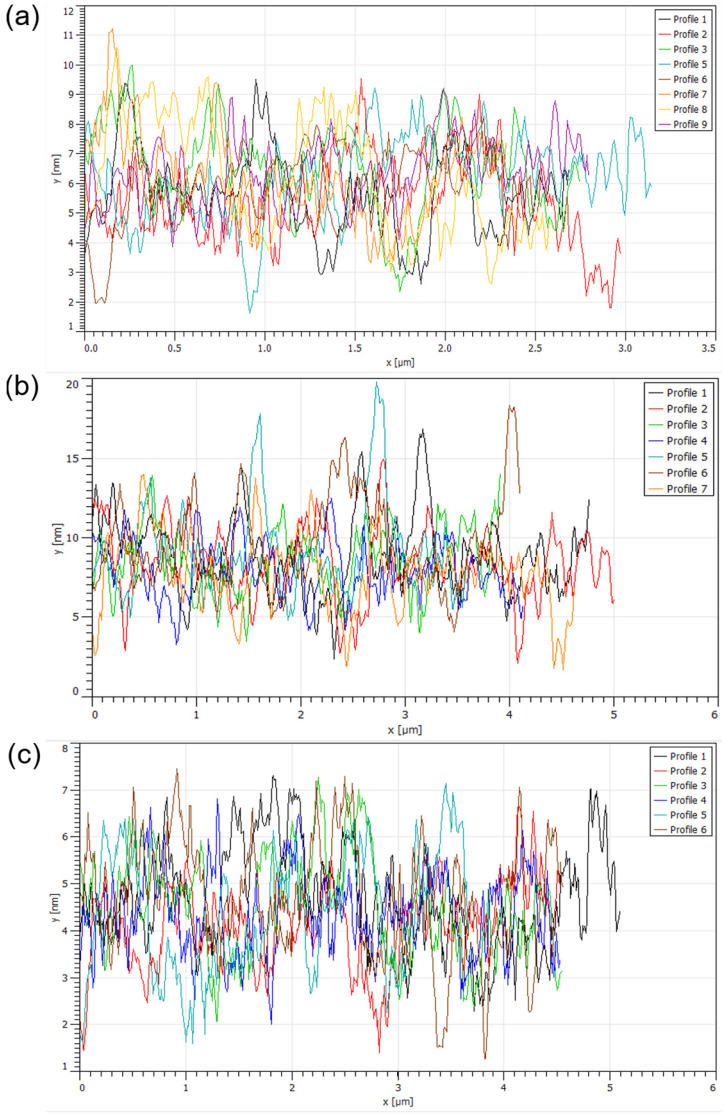

Fig. S7 Arbitrary line scan heigh profiles of the 5 × 5 μm^2 AFM images for (a) PM6:Y-*thio*-EG, (b) PM6:Y-*pyr*-EG, (c) PM6:Y6.

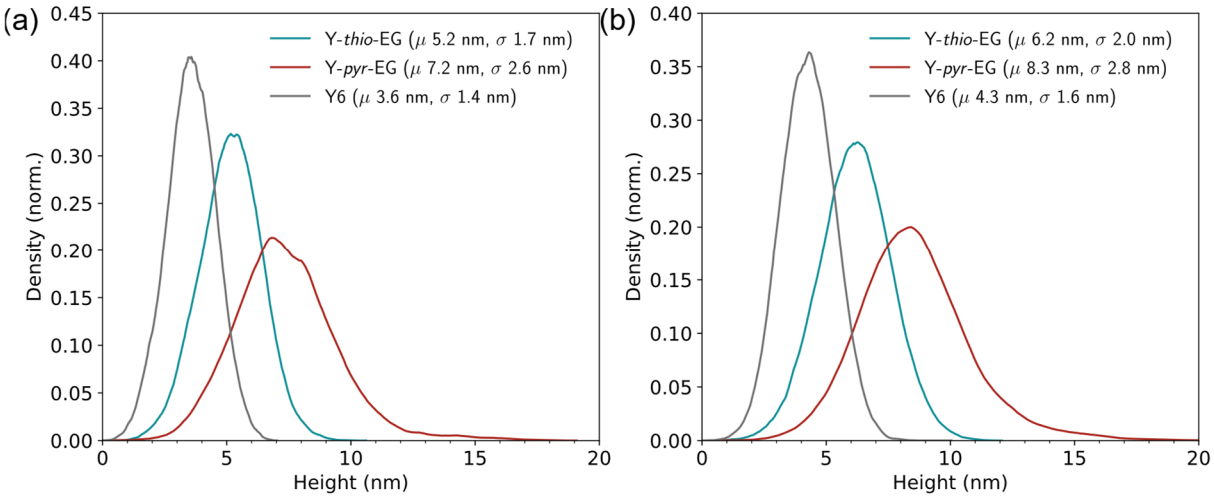

Fig. S8 Height distribution of the (a) 5×5 μm^2 and (b) 2×2 μm^2 AFM images. The mean (μ) and standard deviation (σ) were extracted by Gauss distribution fitting.

NMR & Mass Spectra

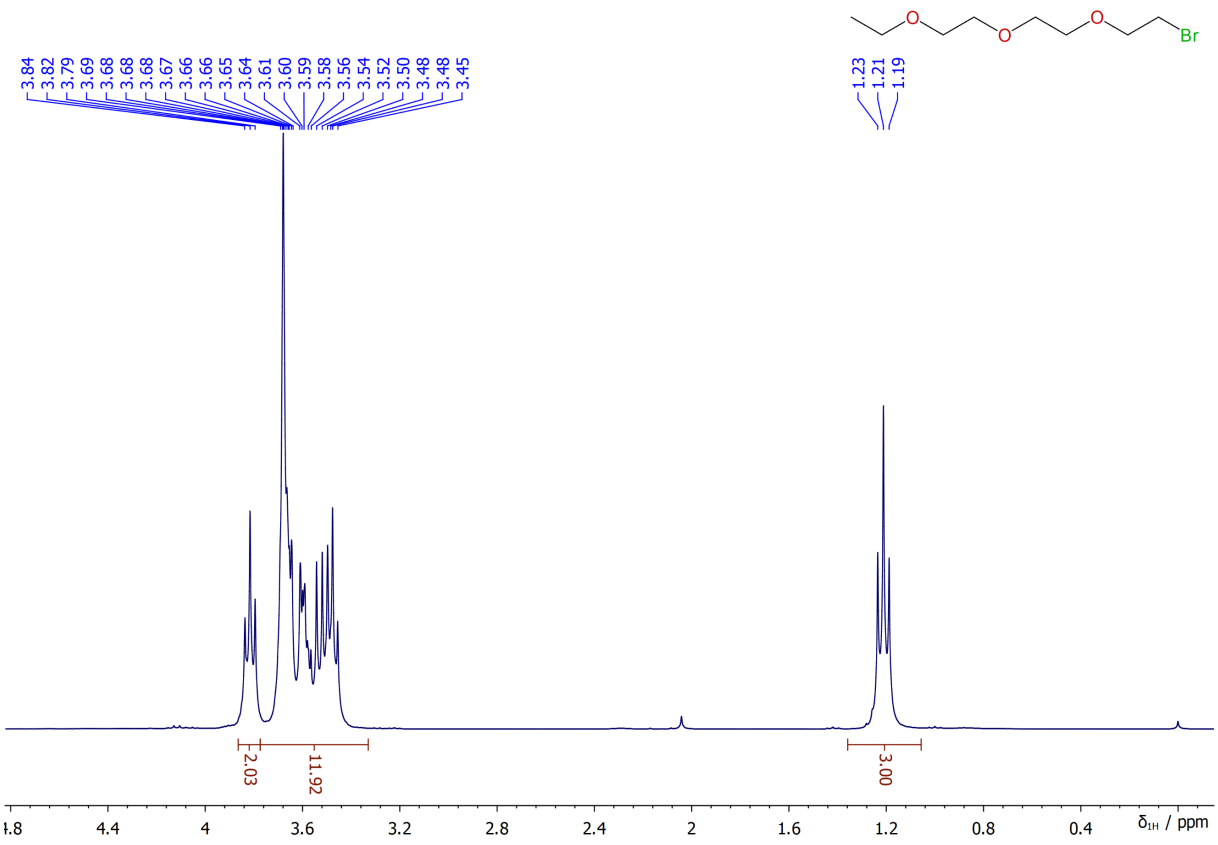

Fig. S9 ^{1}H NMR (300 MHz) spectrum of compound **TEG-Br**.

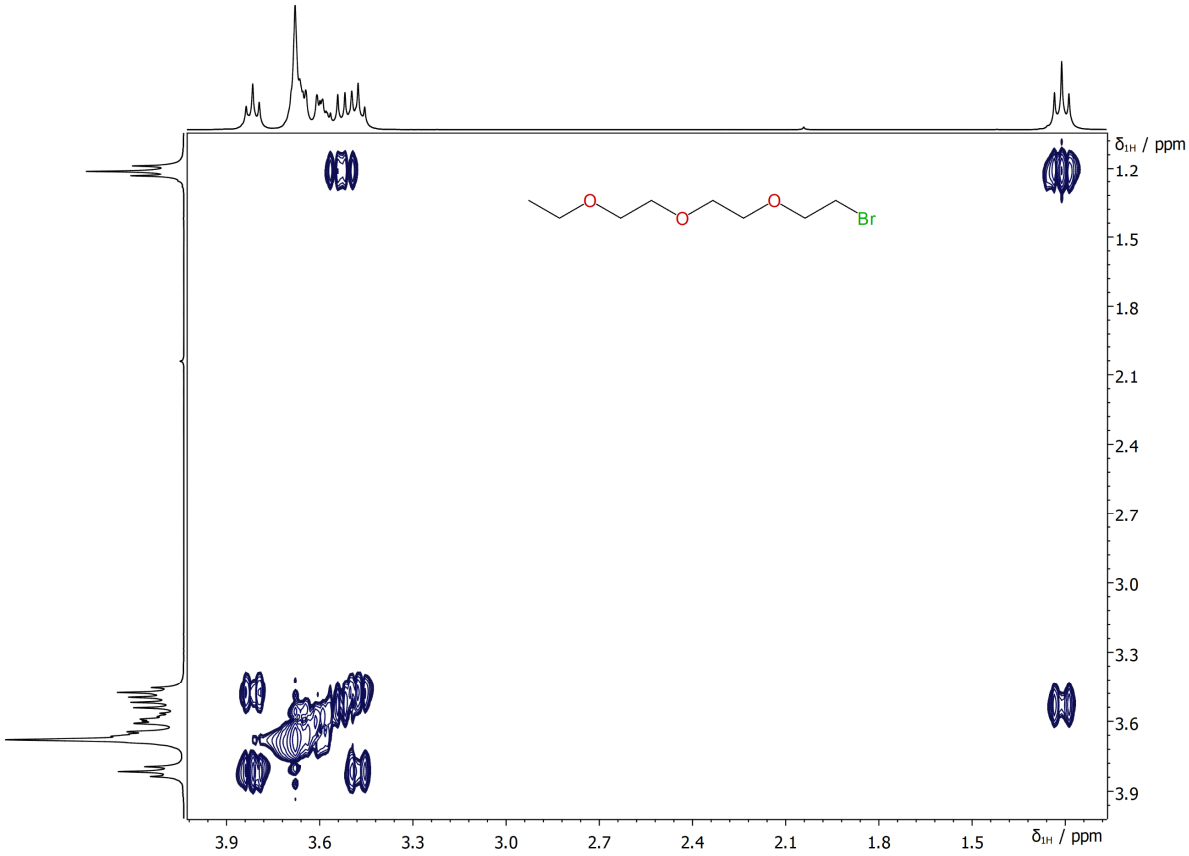

Fig. S10 COSY NMR (300 MHz) spectrum of compound **TEG-Br**.

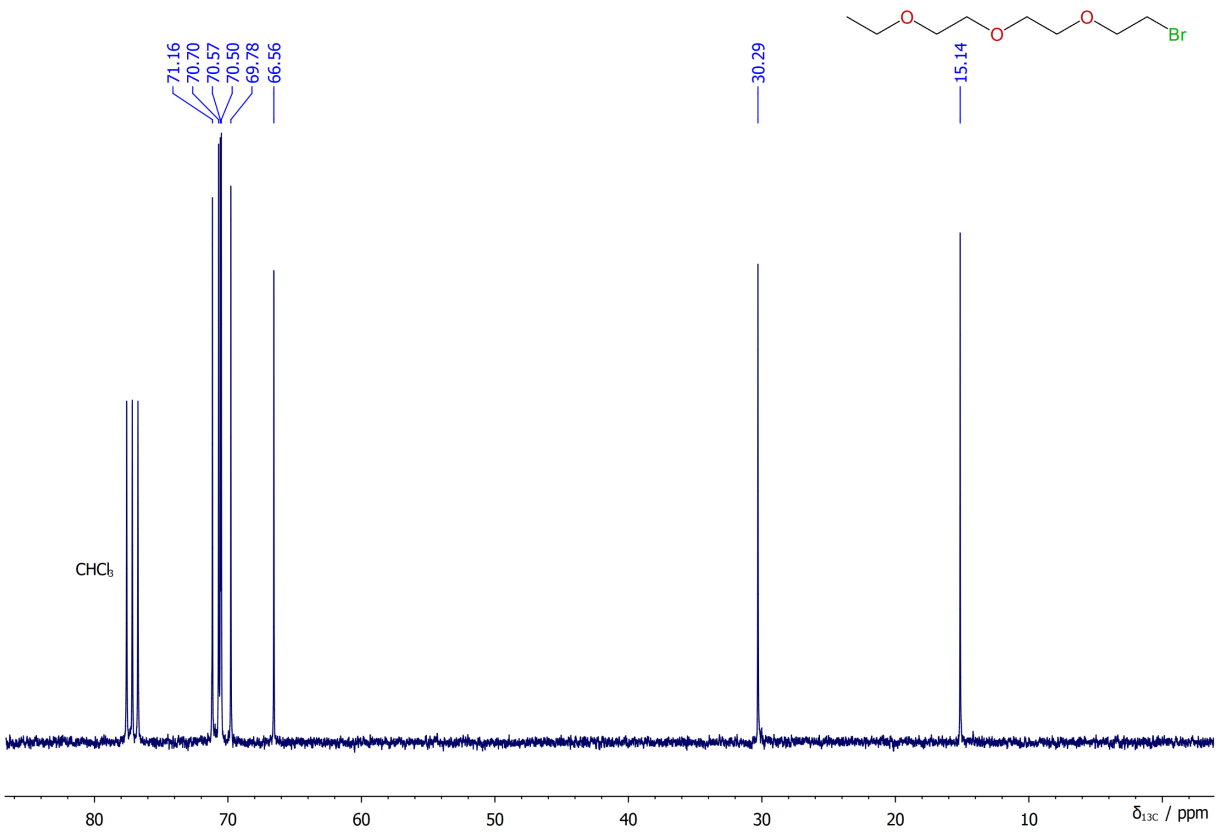

Fig. S11 ^{13}C NMR (75 MHz) spectrum of compound **TEG-Br**.

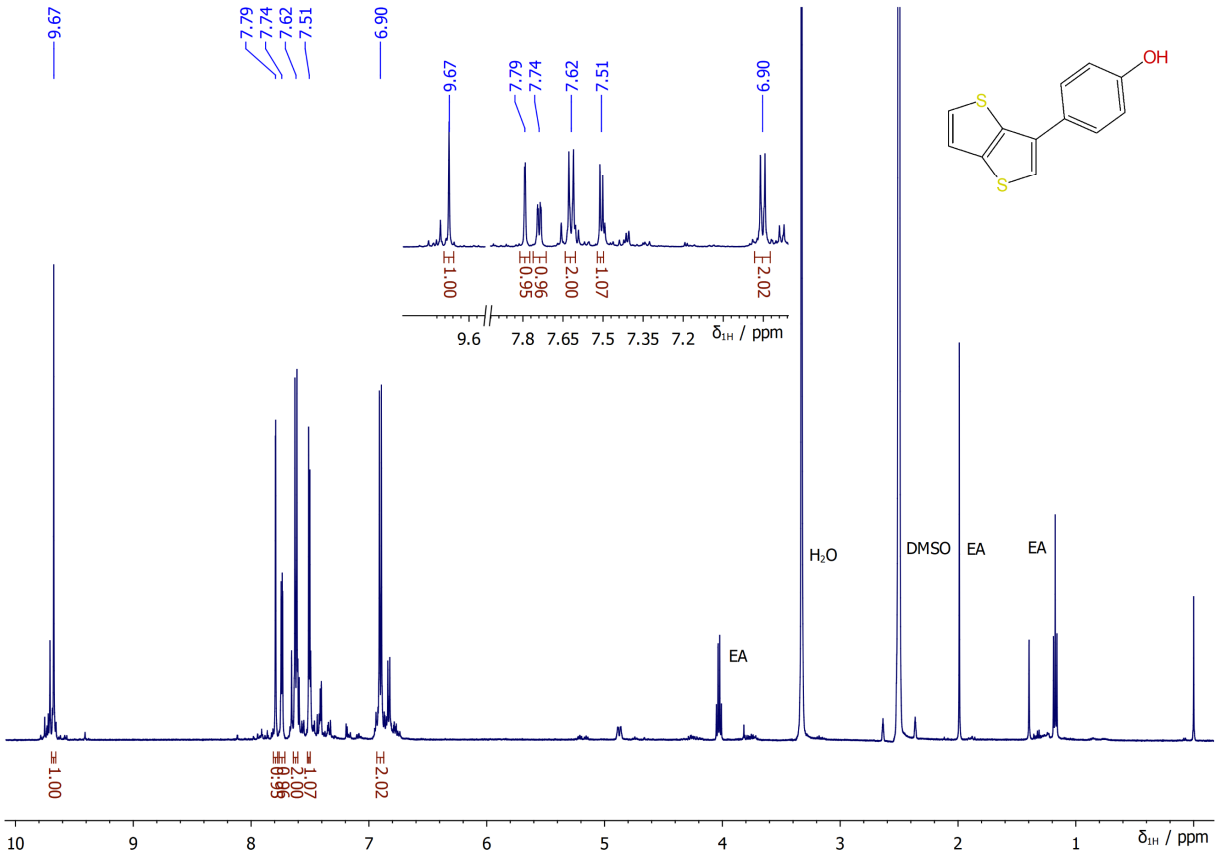

Fig. S12 ^{1}H NMR (500 MHz) spectrum of compound **4**.

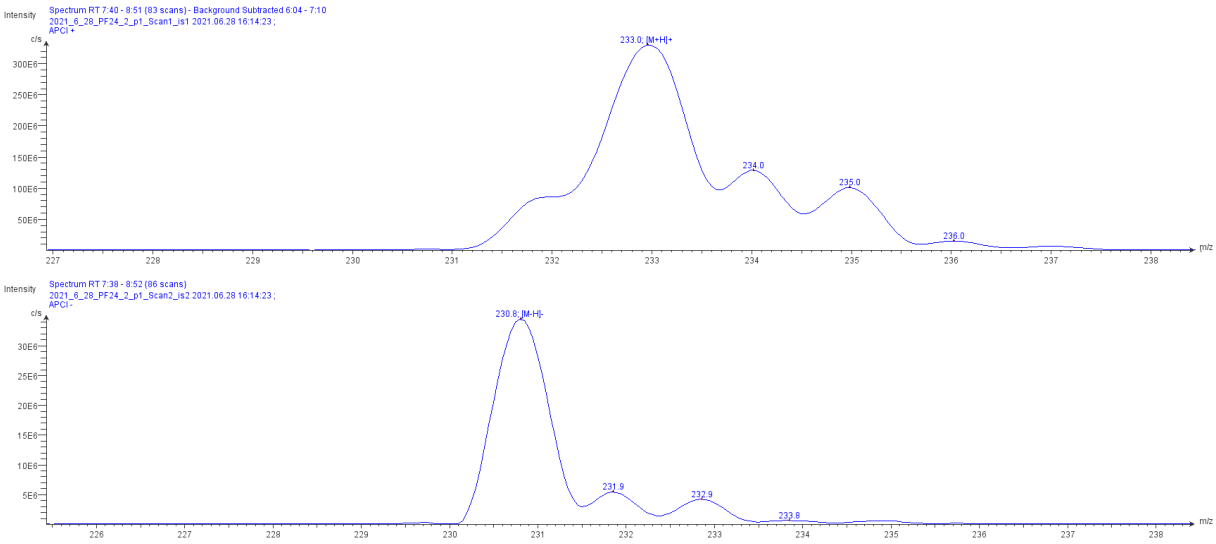

Fig. S13 APCI-MS spectrum of compound **4**.

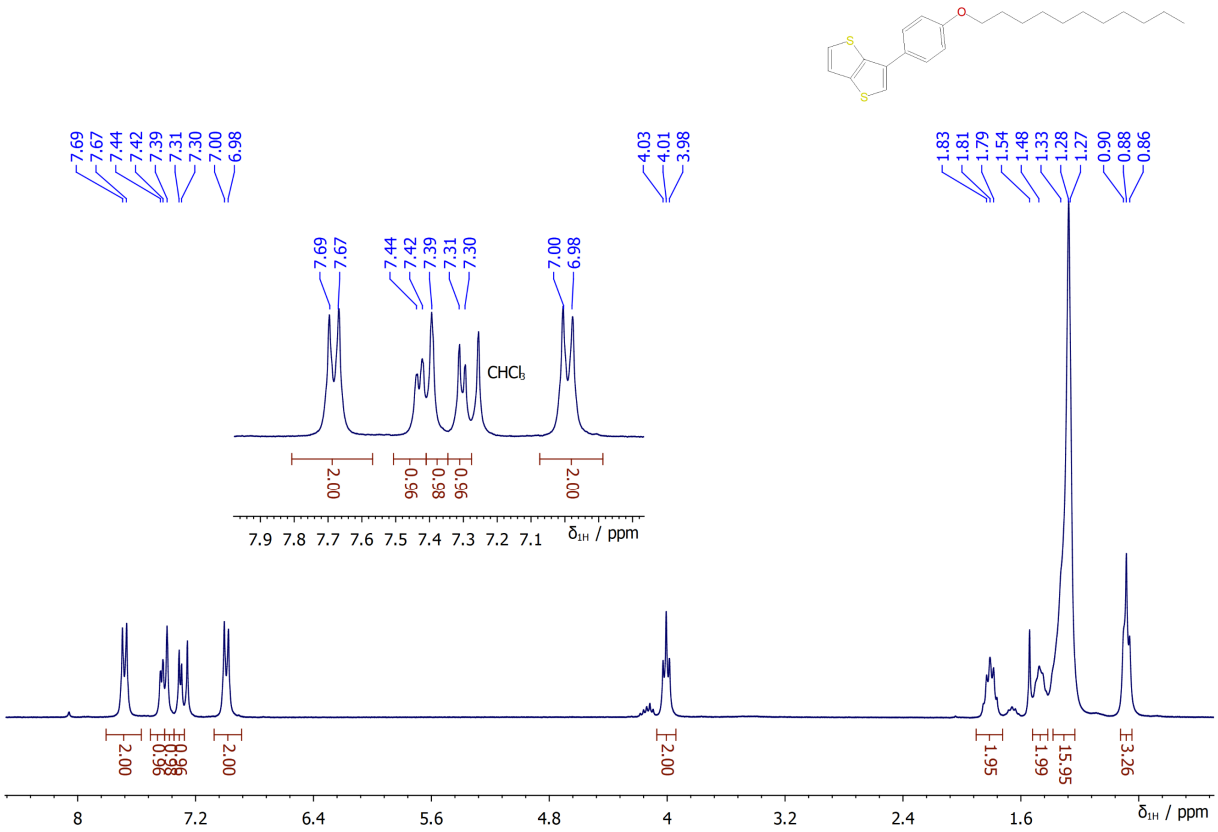

Fig. S14 ^{1}H NMR (300 MHz) spectrum of compound **5a**.

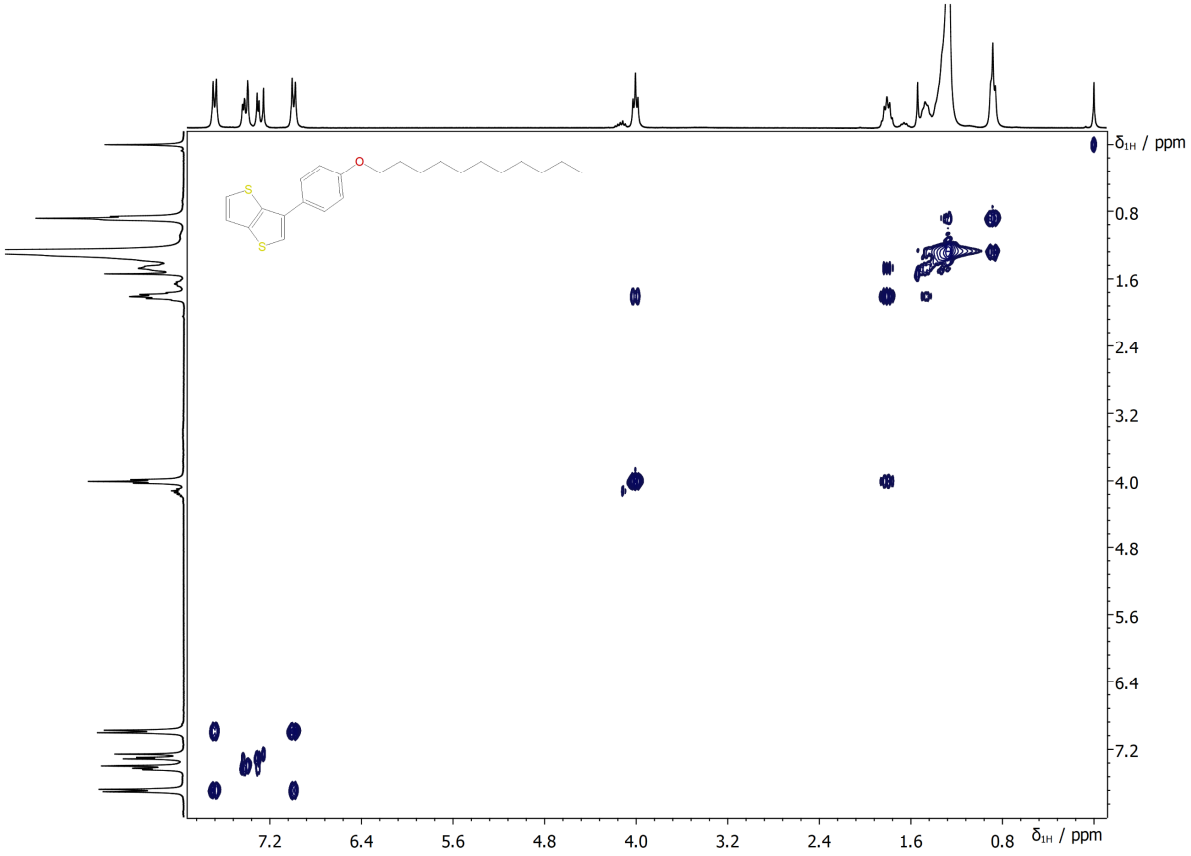

Fig. S15 COSY NMR (300 MHz) spectrum of compound **5a**.

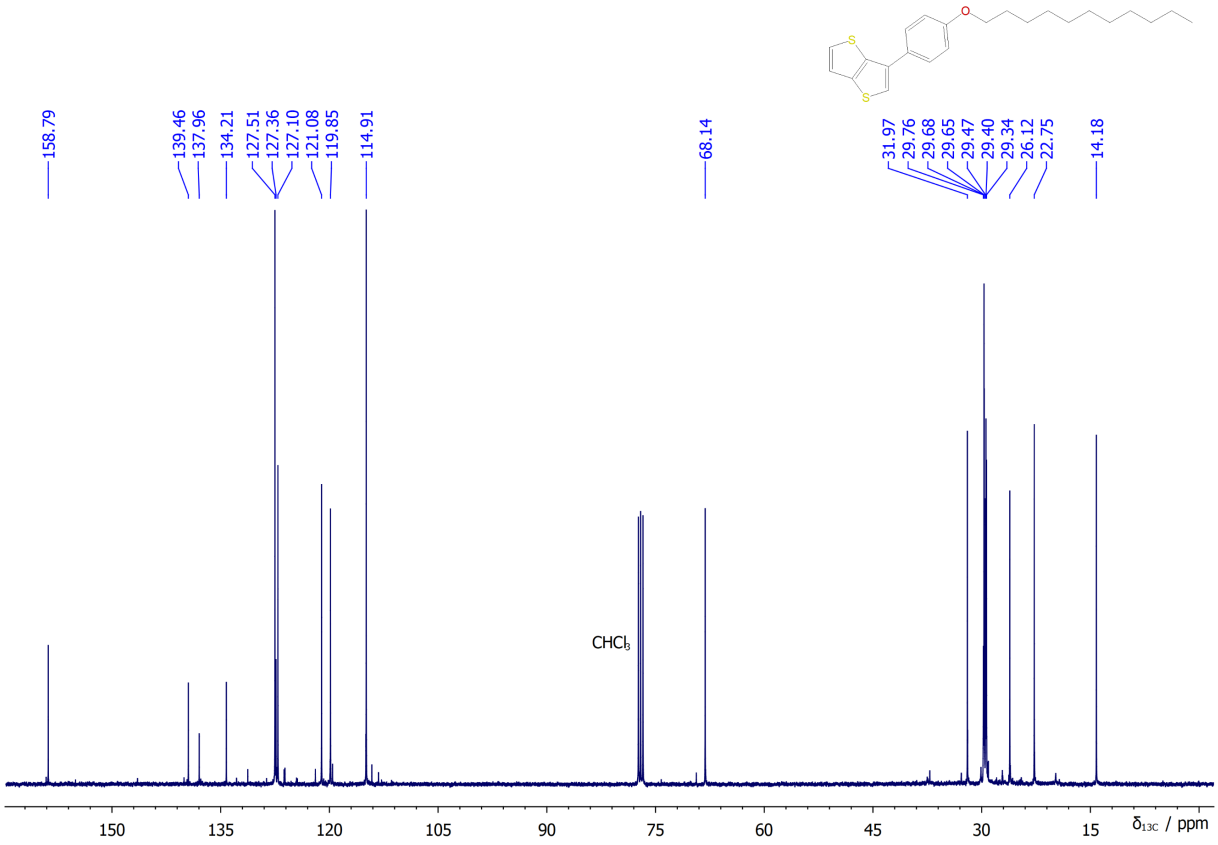

Fig. S16 ^{13}C NMR (100 MHz) spectrum of compound **5a**.

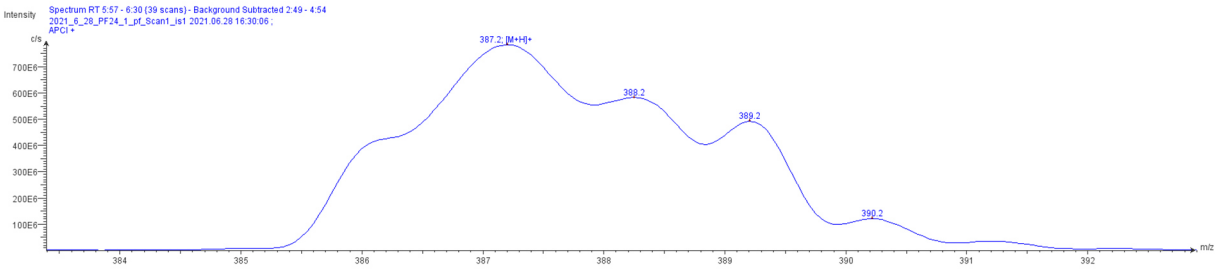

Fig. S17 APCI-MS spectrum of compound **5a**.

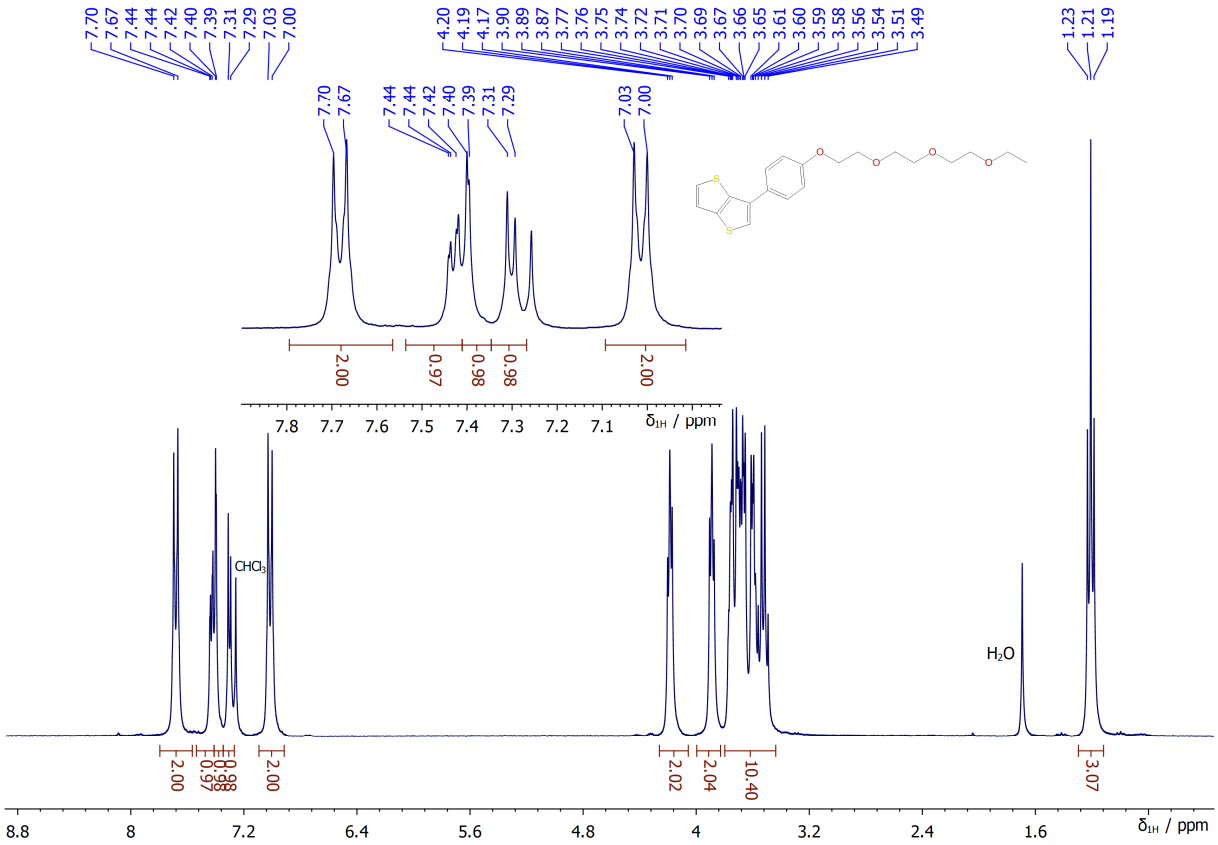

Fig. S18 ^{1}H NMR (300 MHz) spectrum of compound **5b**.

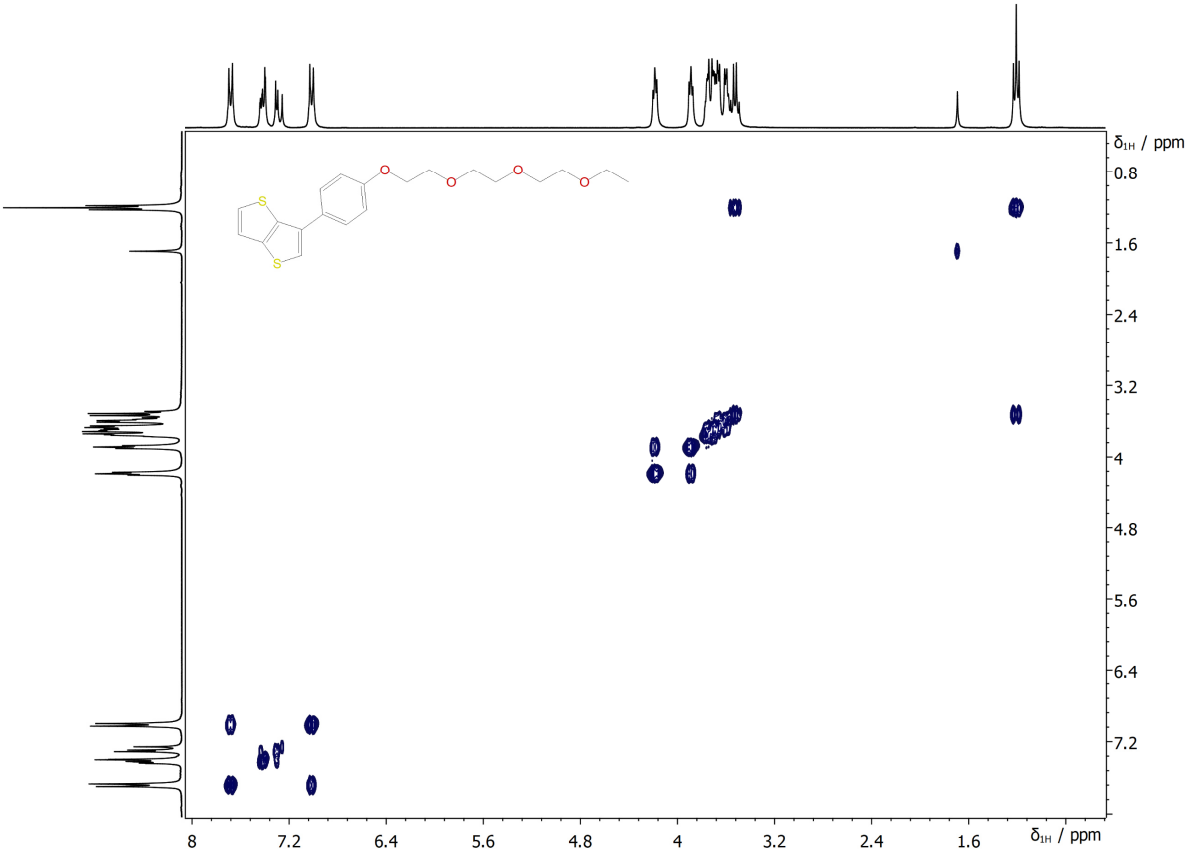

Fig. S19 COSY NMR (300 MHz) spectrum of compound **5b**.

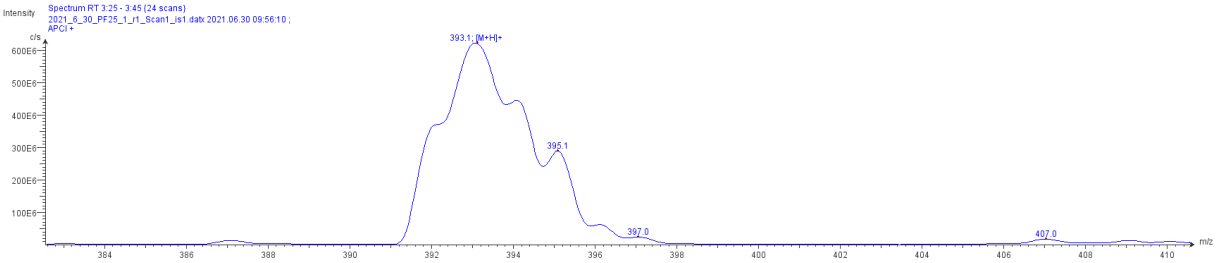

Fig. S20 APCI-MS spectrum of compound **5b**.

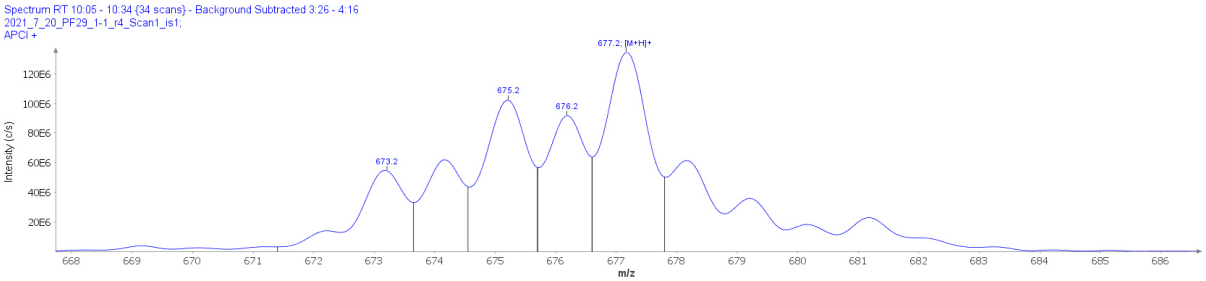

Fig. 21 APCI-MS spectrum of compound **6a**.

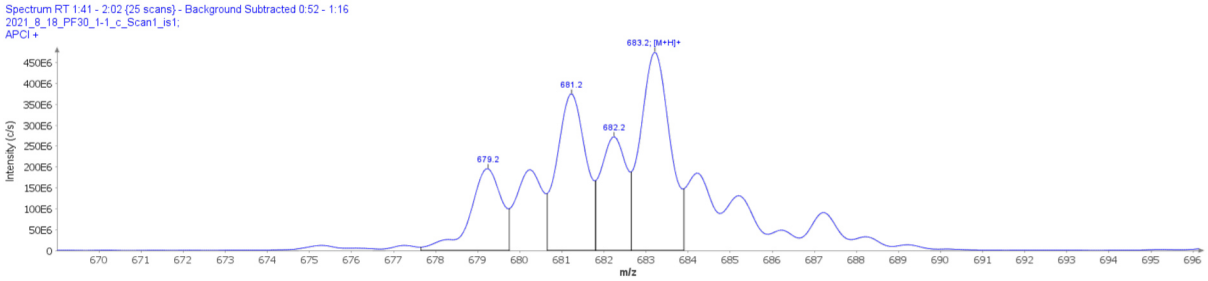

Fig. S22 APCI-MS spectrum of compound **6b**.

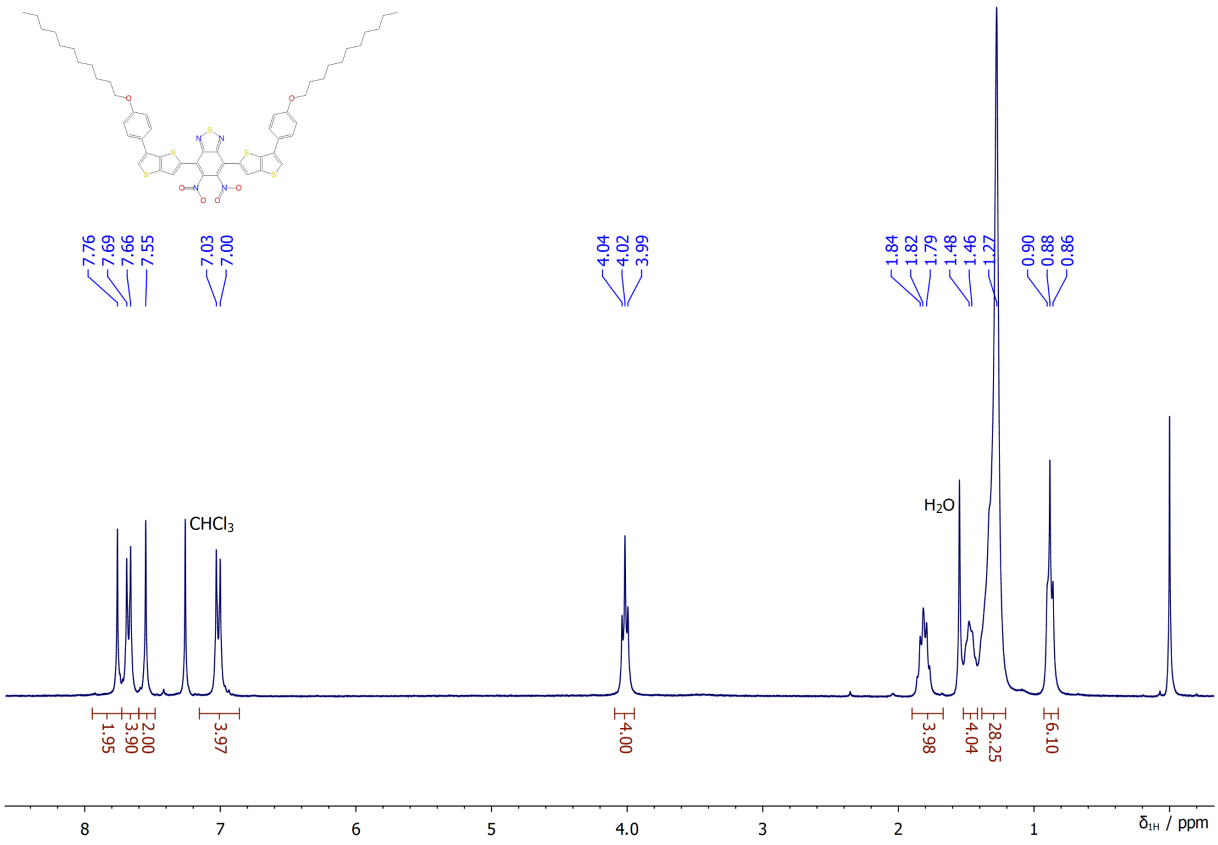

Fig. S23 ^{1}H NMR (300 MHz) spectrum of compound **7a**.

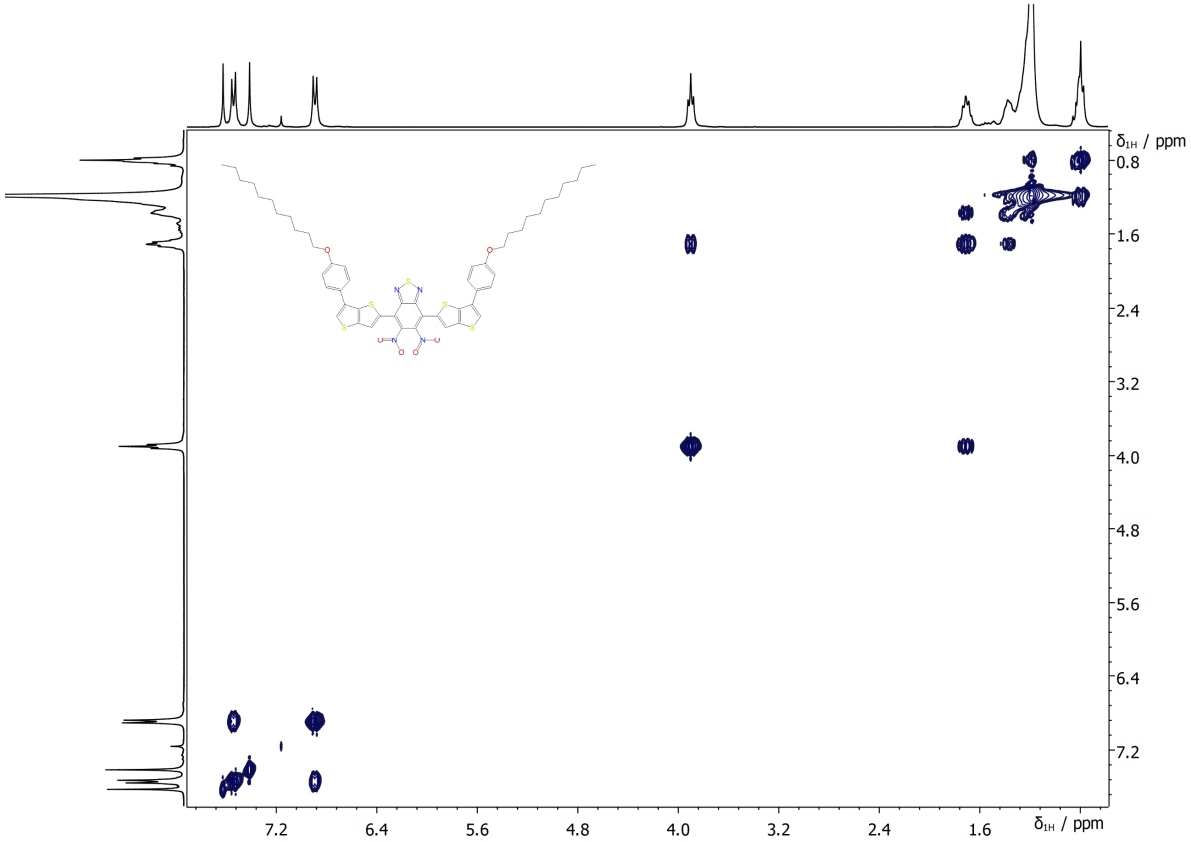

Fig. S24 COSY NMR (300 MHz) spectrum of compound **7a**.

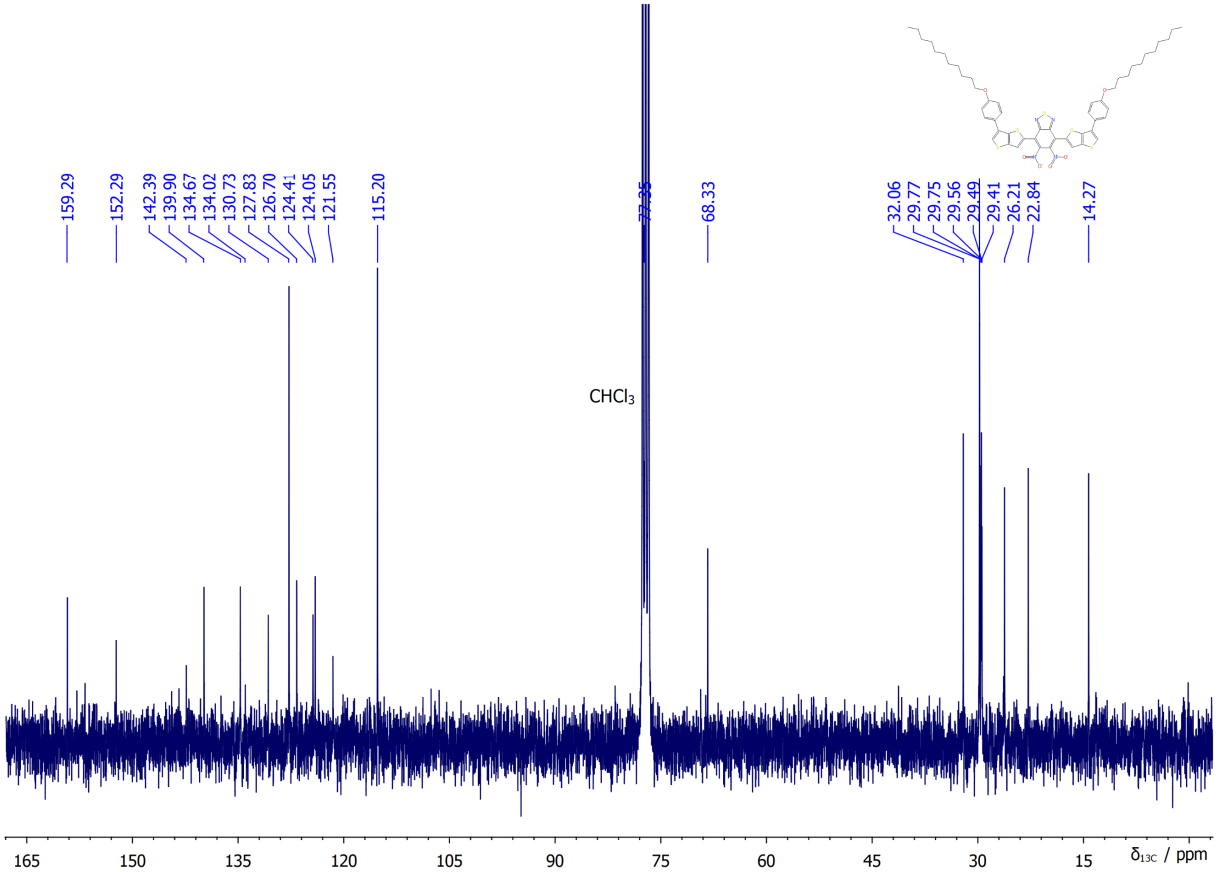

Fig. S25 ^{13}C NMR (75 MHz) spectrum of compound **7a**.

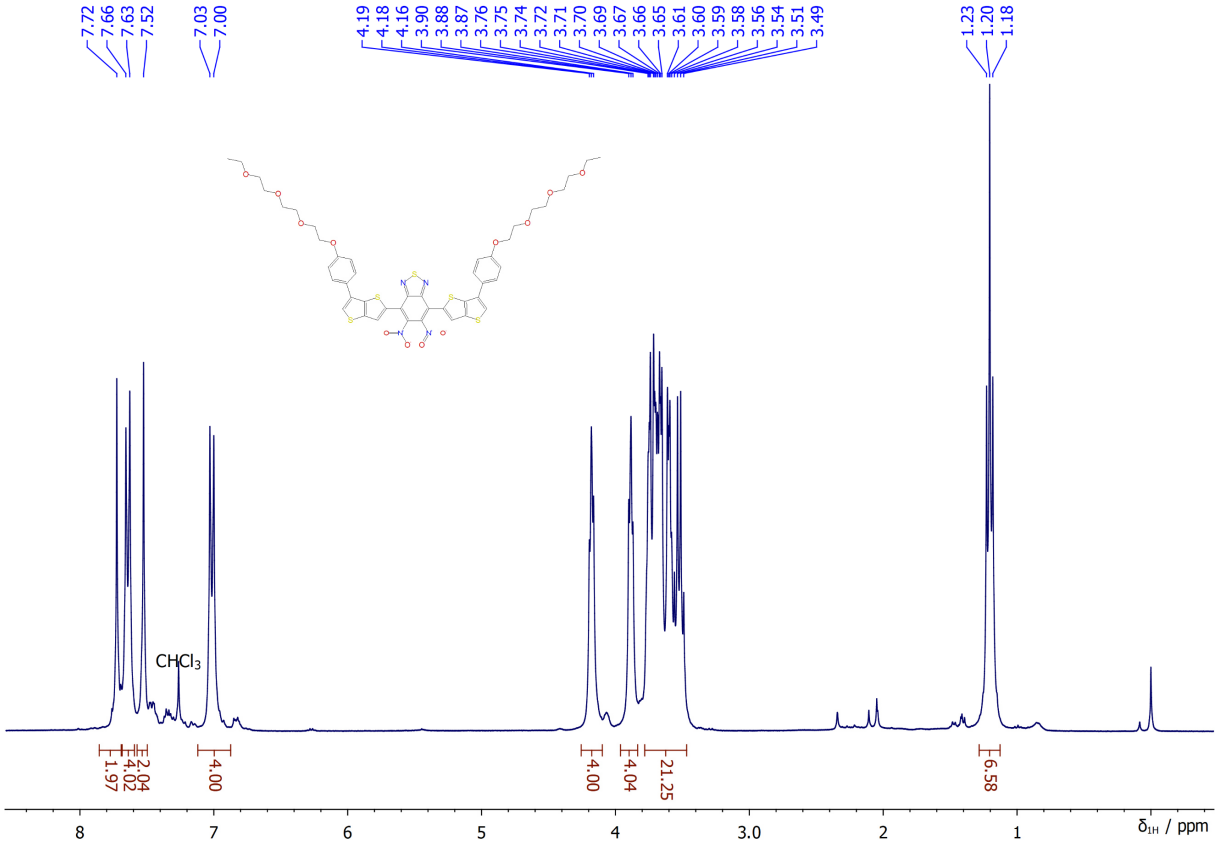

Fig. S26 ^{1}H NMR (300 MHz) spectrum of compound **7b**.

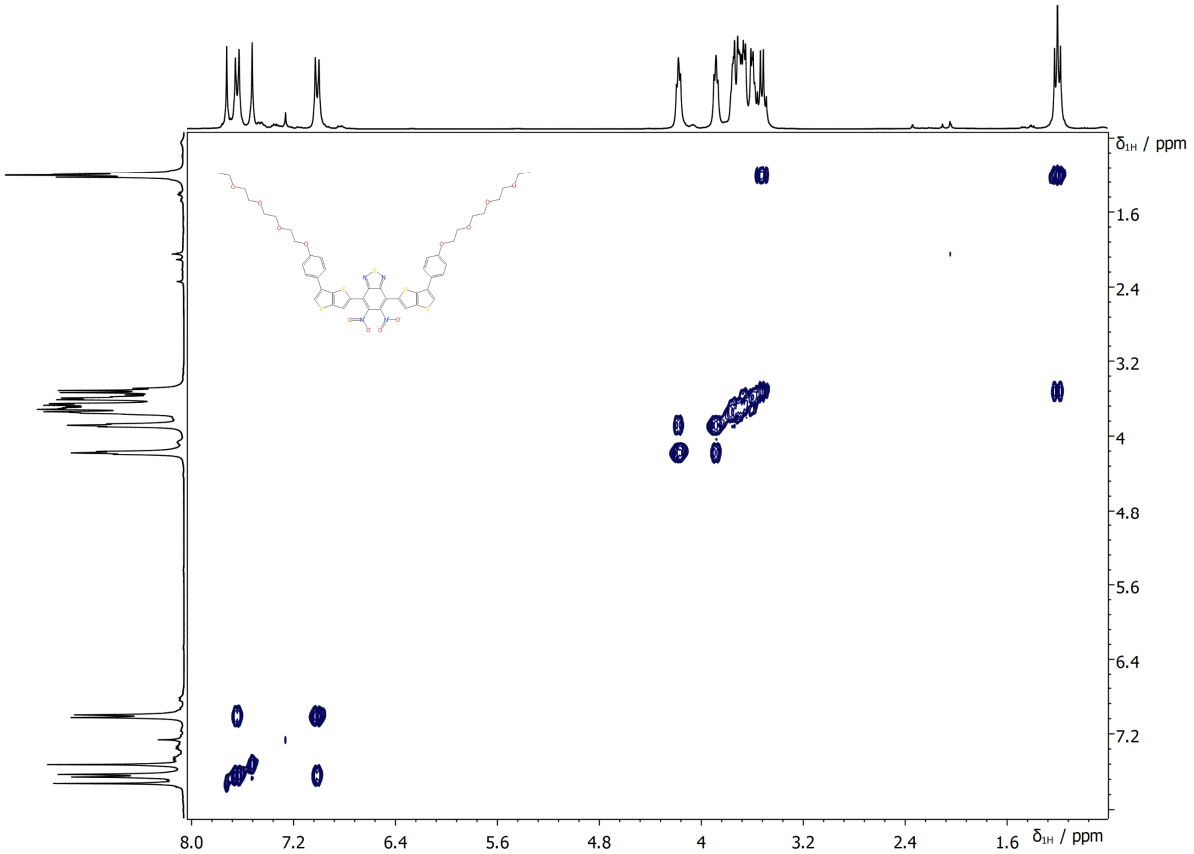

Fig. S27 COSY NMR (300 MHz) spectrum of compound **7b**.

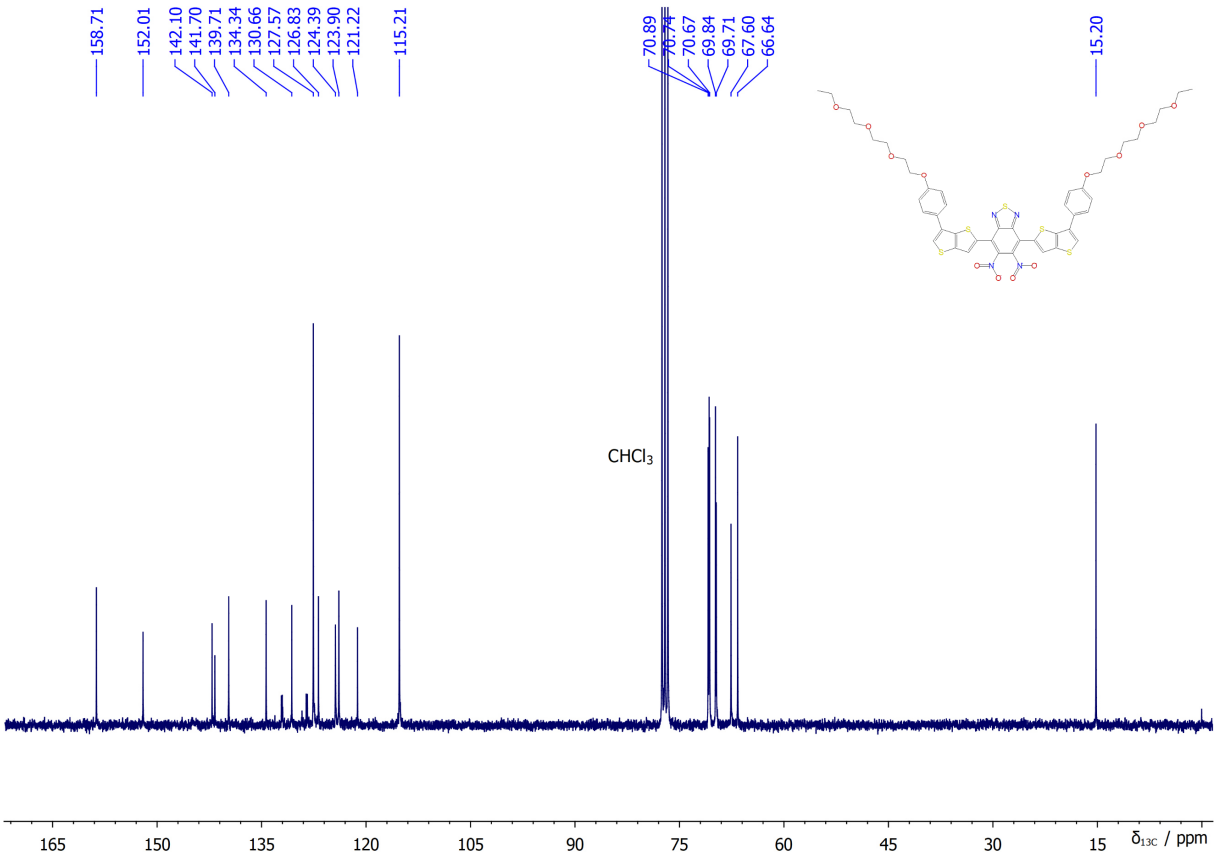

Fig. S28 ^{13}C NMR (75 MHz) spectrum of compound **7b**.

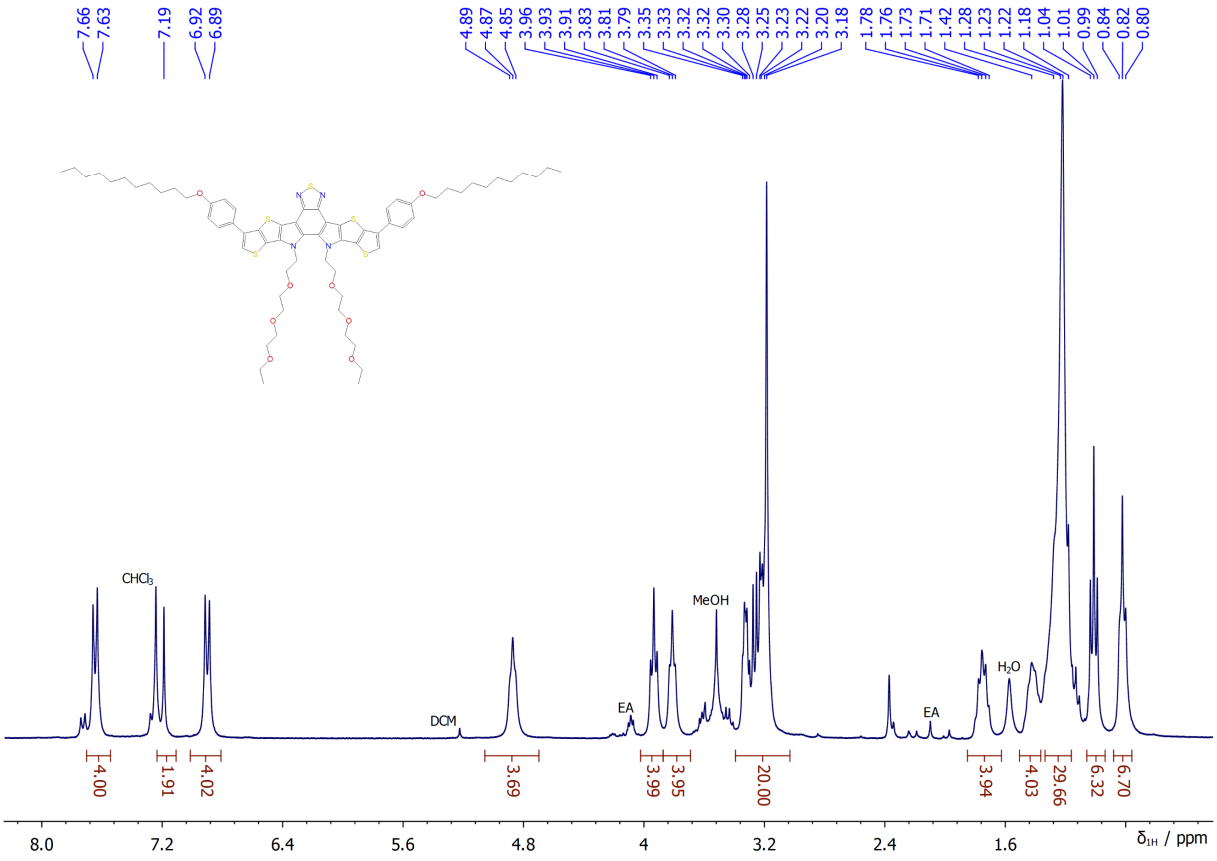

Fig. S29 ^{1}H NMR (300 MHz) spectrum of compound **9a**.

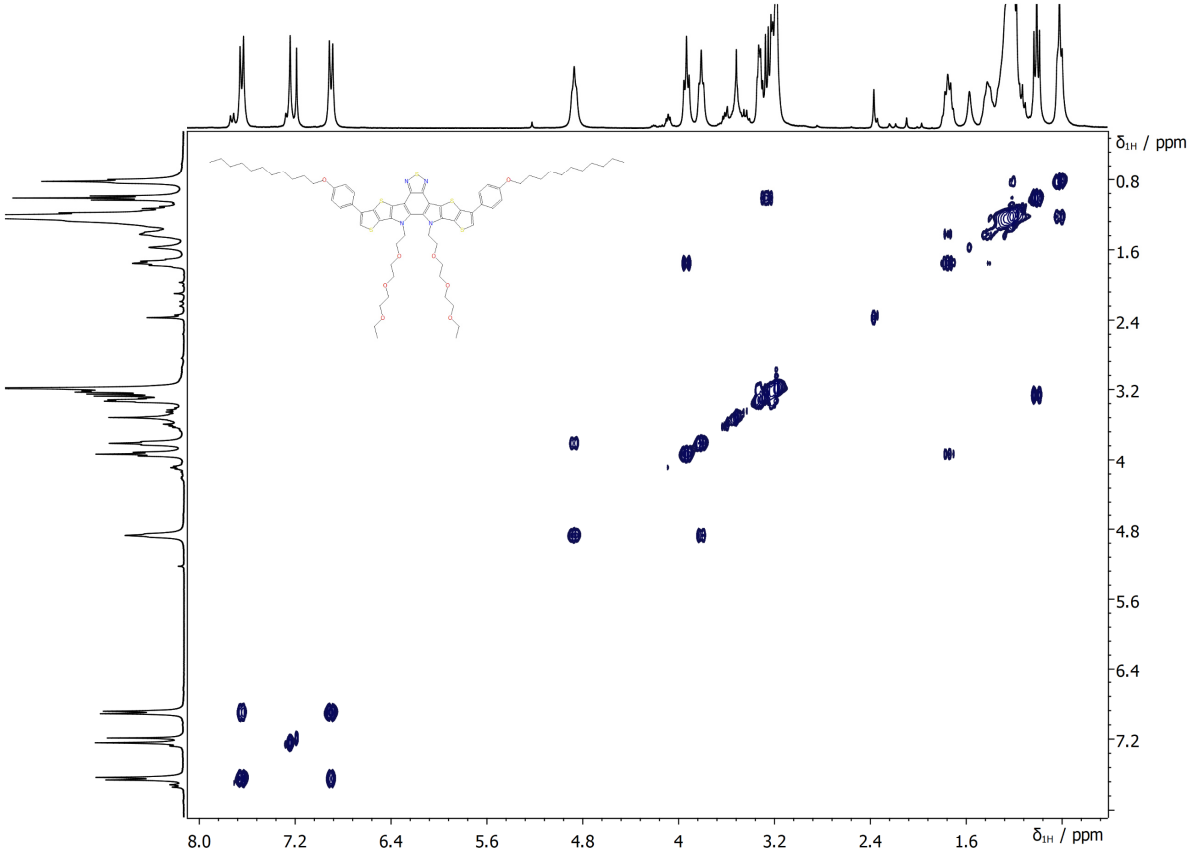

Fig. S30 COSY NMR (300 MHz) spectrum of compound **9a**.

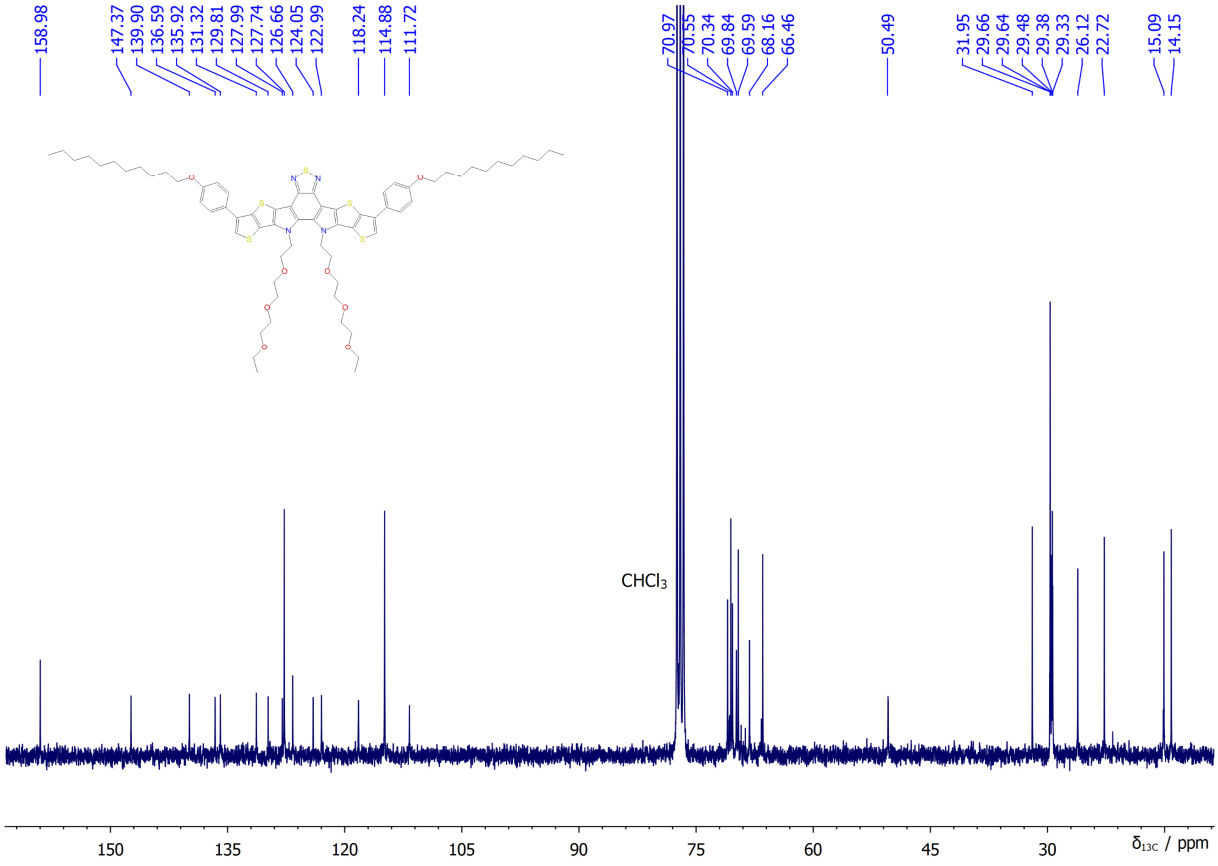

Fig. S31 ^{13}C NMR (75 MHz) spectrum of compound **9a**.

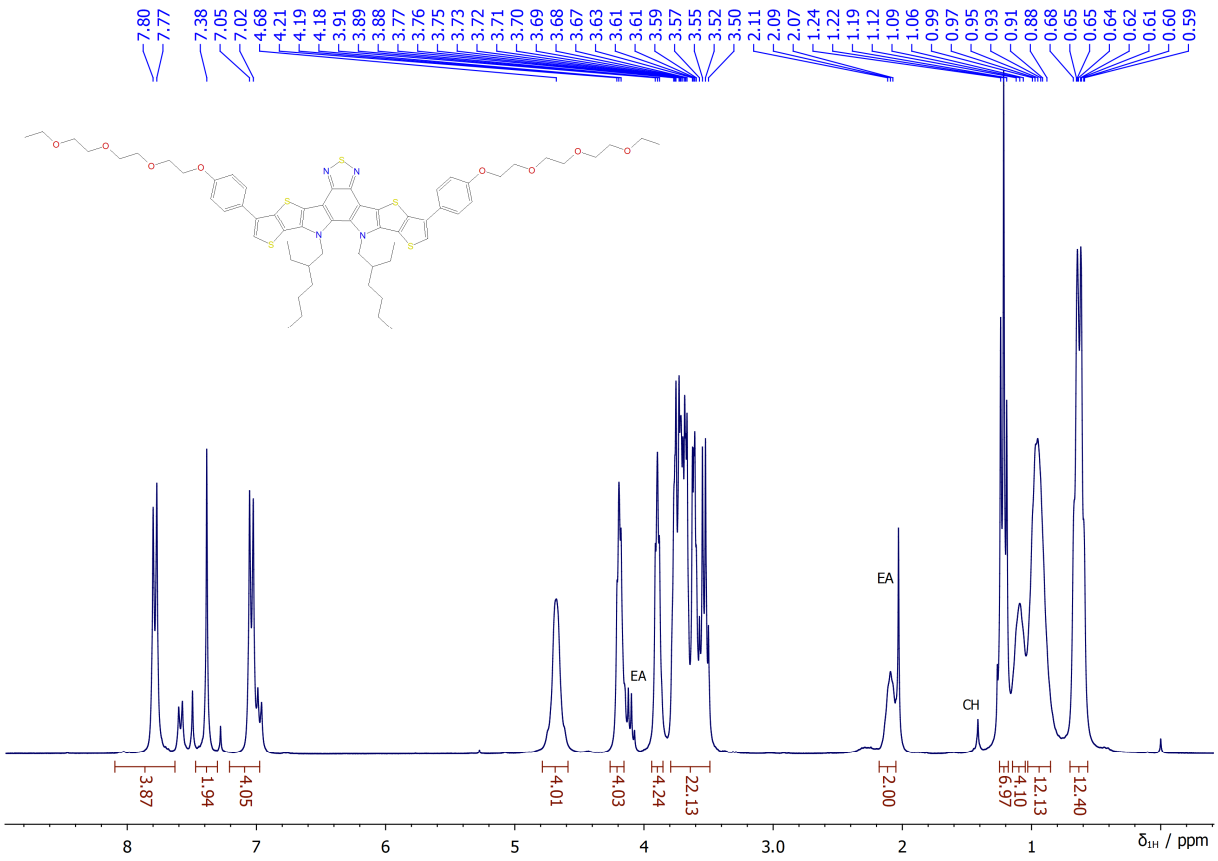

Fig. S32 ^{1}H NMR (300 MHz) spectrum of compound **9b**.

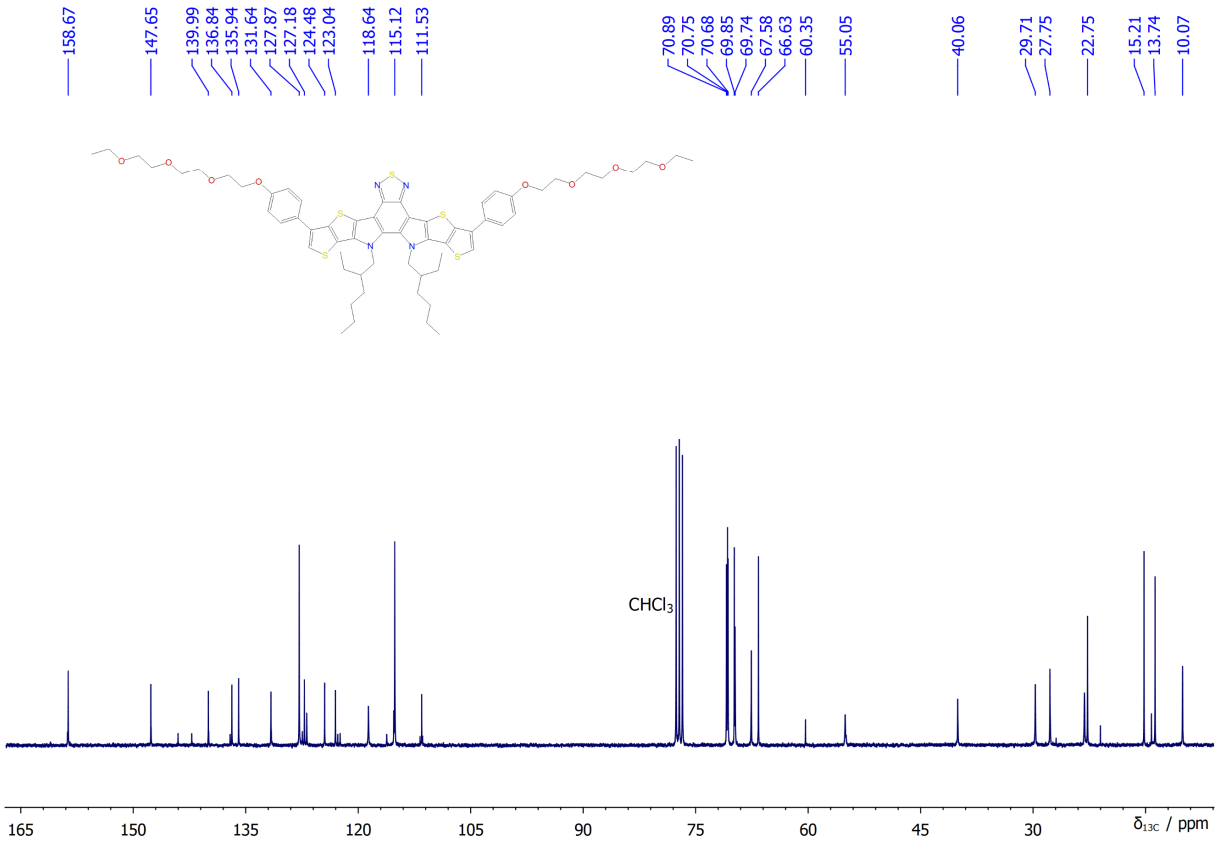

Fig. S33 ^{13}C NMR (75 MHz) spectrum of compound **9b**.

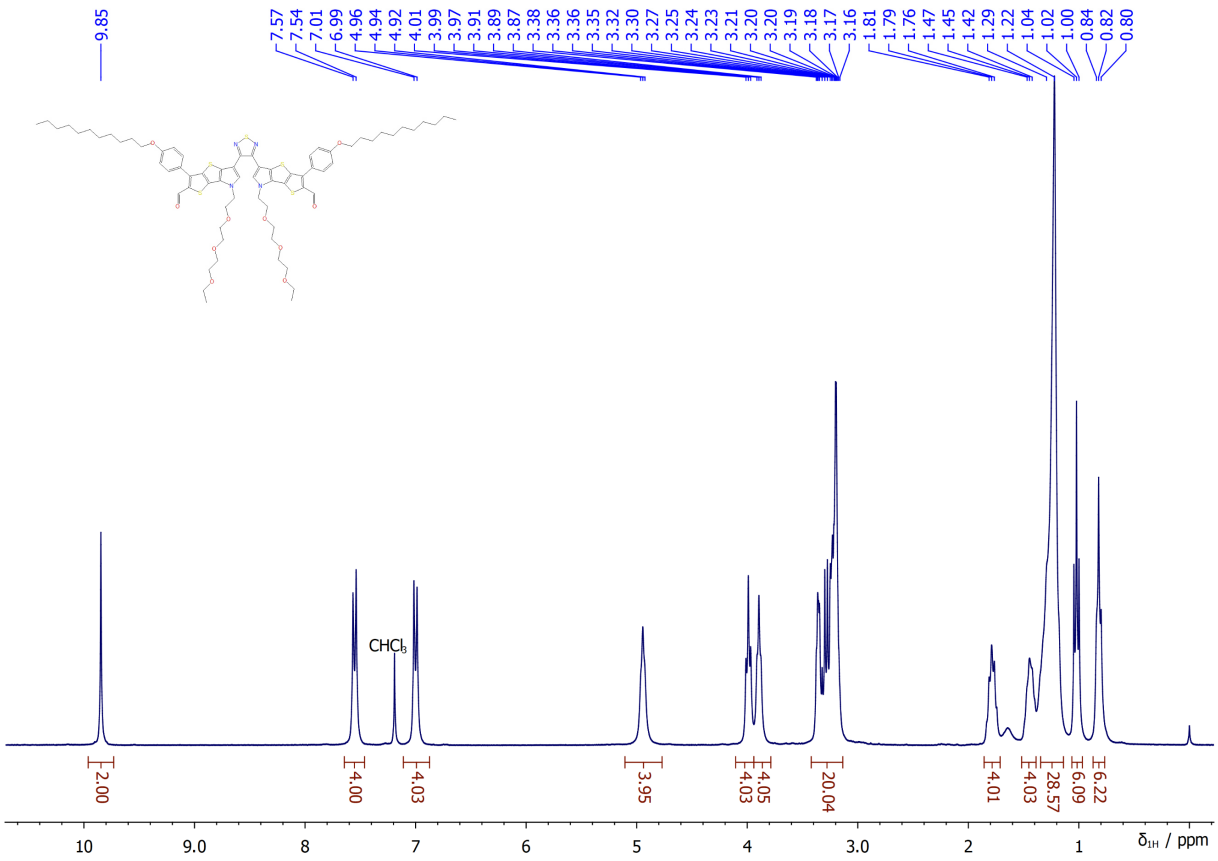

Fig. S34 ^{1}H NMR (300 MHz) spectrum of compound **10a**.

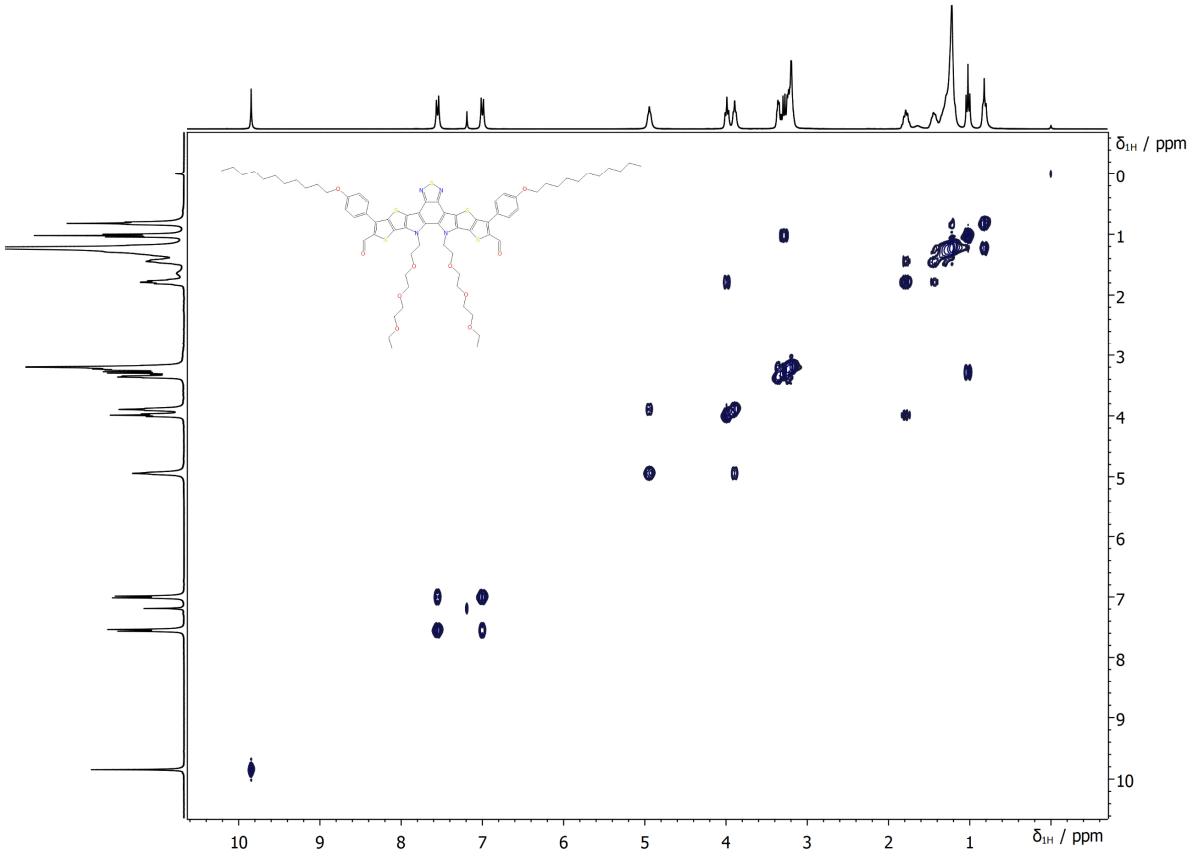

Fig. S35 COSY NMR (300 MHz) spectrum of compound **10a**.

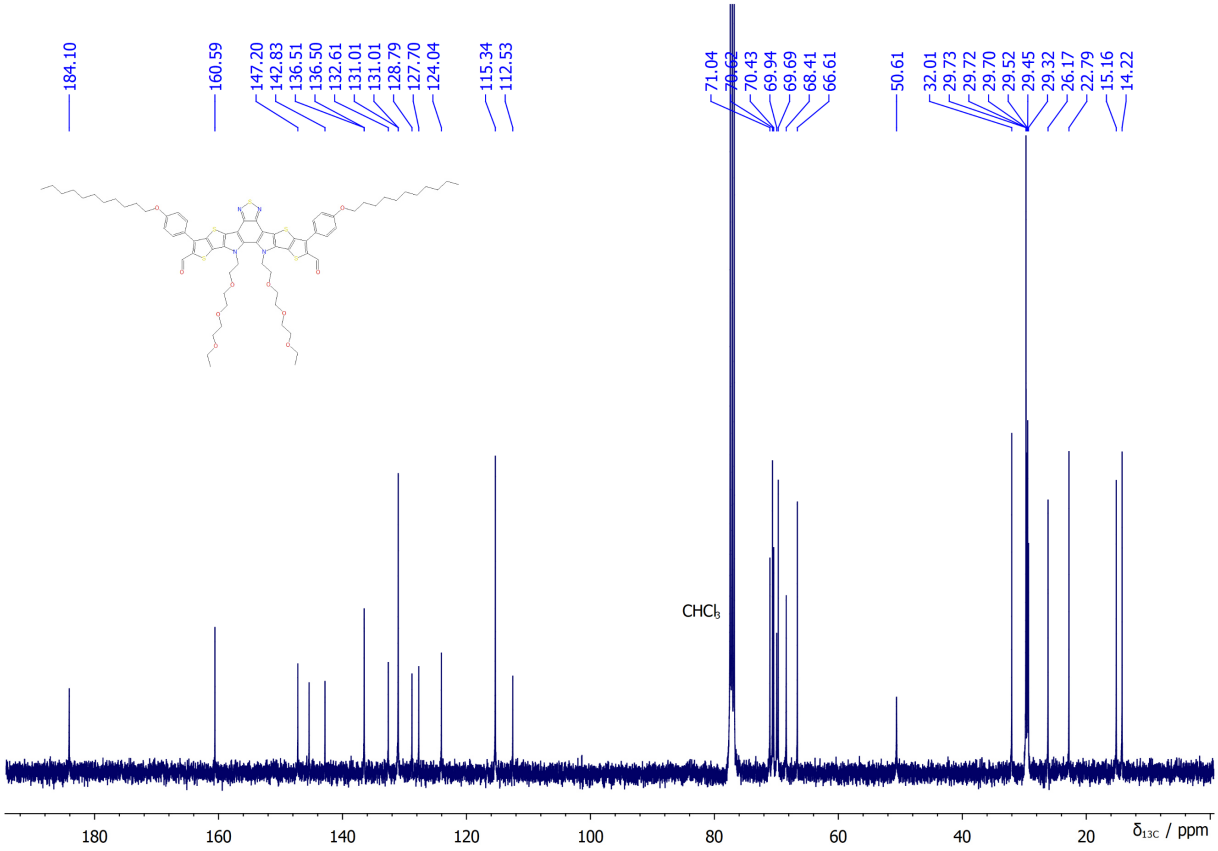

Fig. S36 ^{13}C NMR (100 MHz) spectrum of compound **10a**.

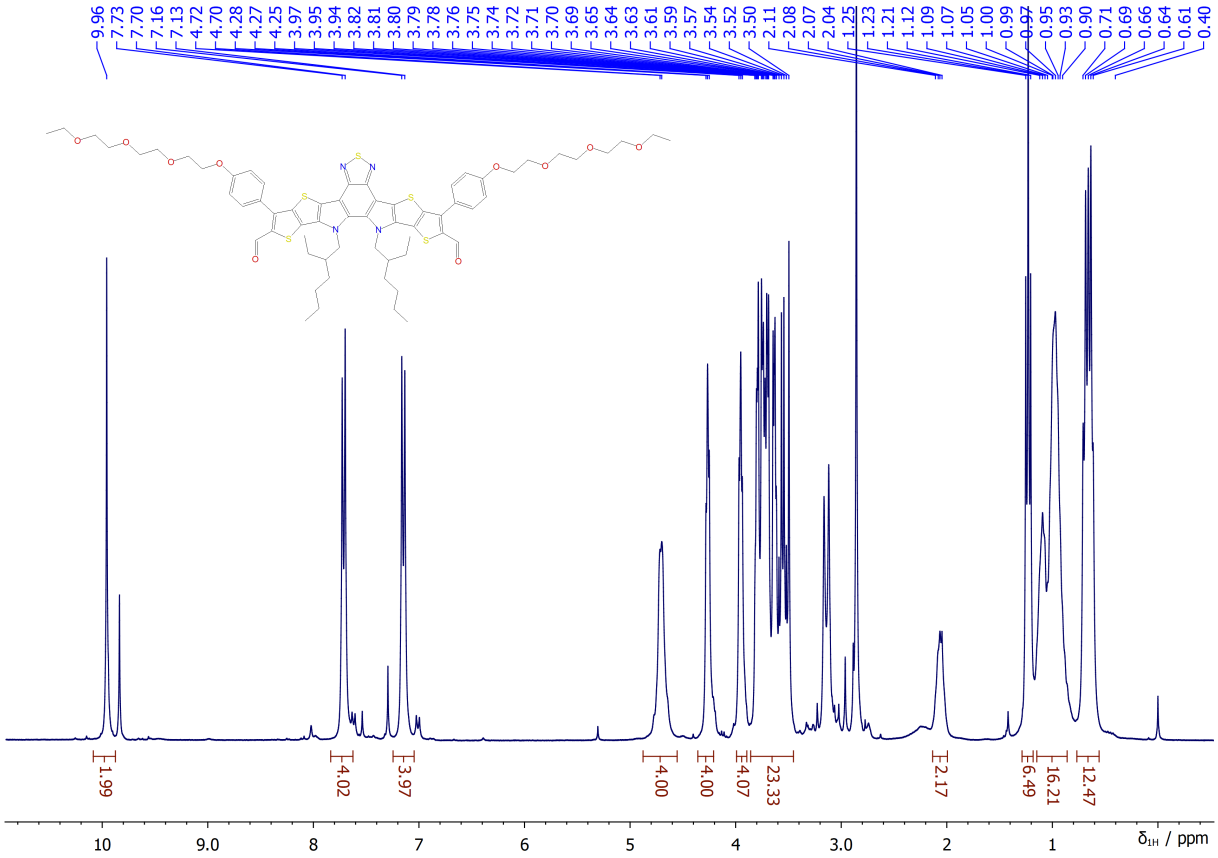

Fig. S37 ^{1}H NMR (300 MHz) spectrum of compound **10b**.

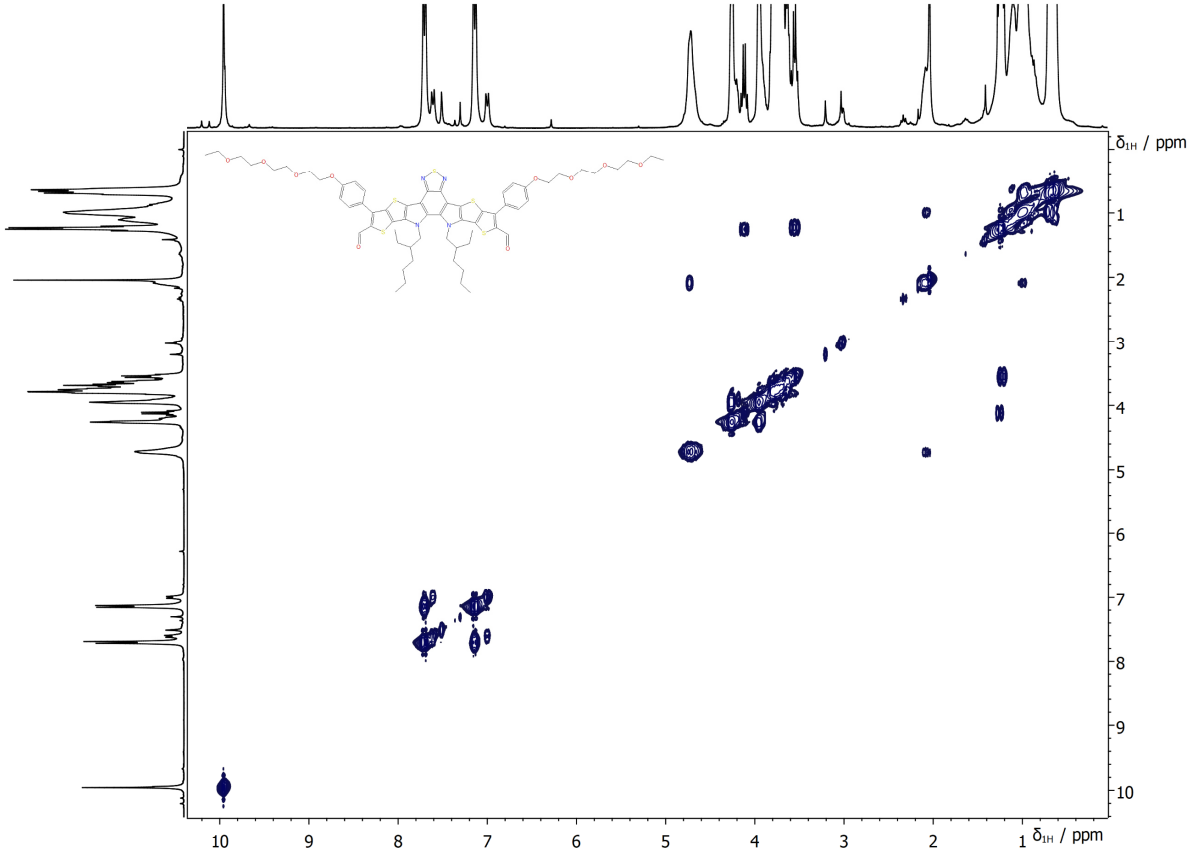

Fig. S38 COSY NMR (300 MHz) spectrum of compound **10b**.

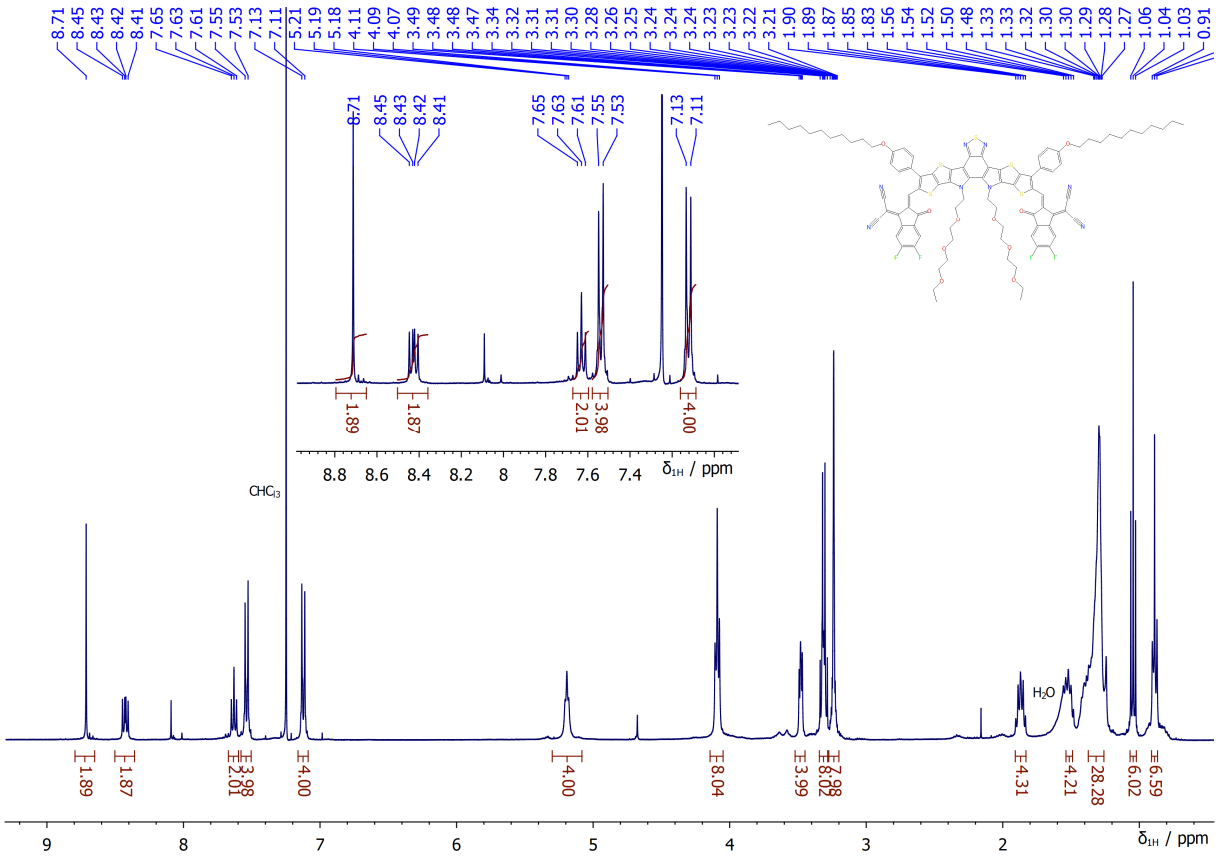

Fig. S39 ^{1}H NMR (400 MHz) spectrum of compound **Y-*pyr*-EG**.

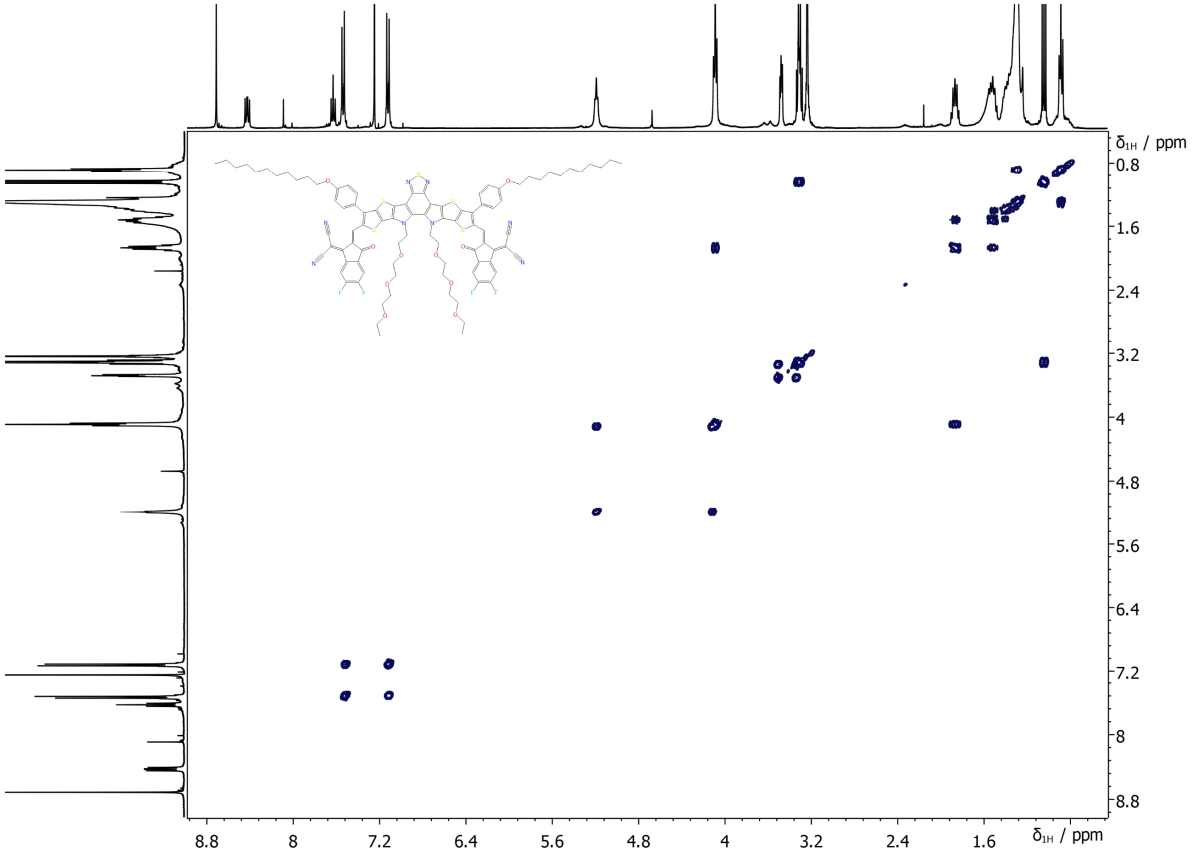

Fig. S40 COSY NMR (400 MHz) spectrum of compound **Y-*pyr*-EG**.

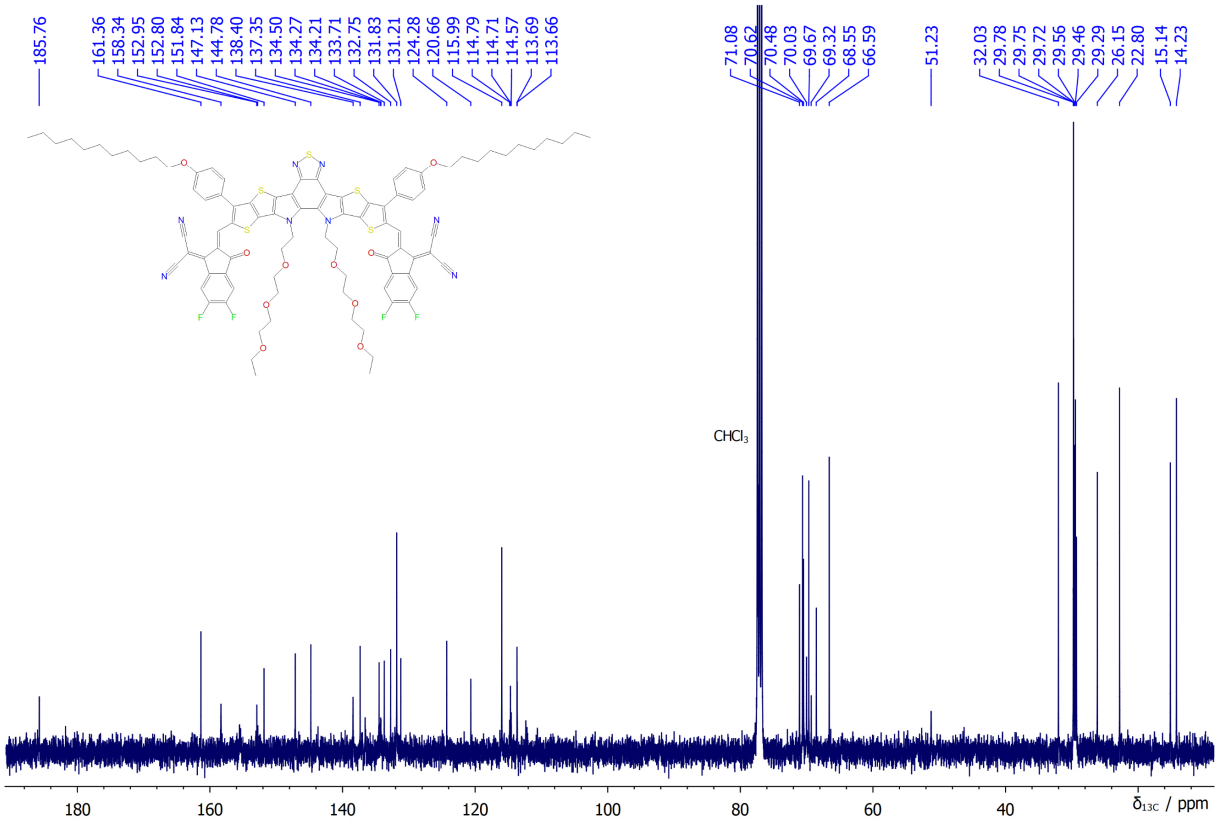

Fig. S41 ^{13}C NMR (100 MHz) spectrum of compound **Y-*pyr*-EG**.

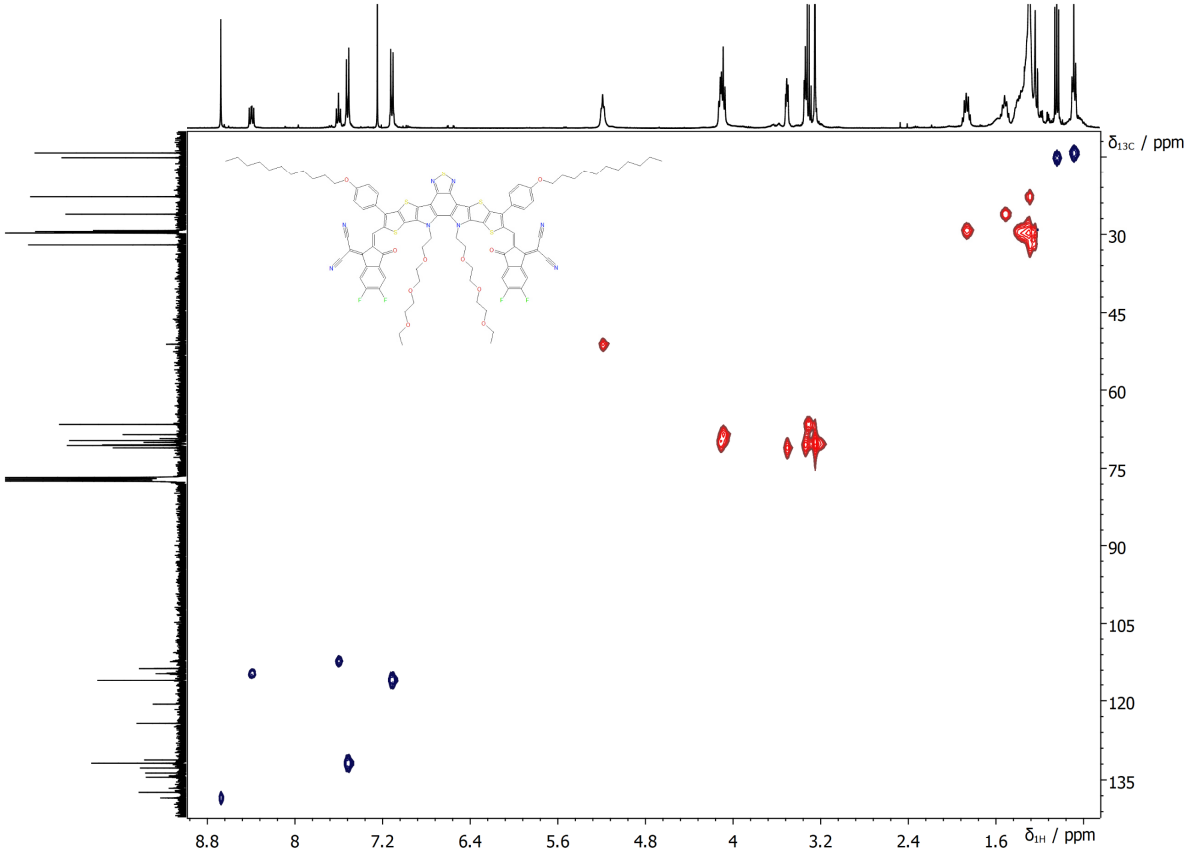

Fig. S42 HSQC NMR (400 MHz) spectrum of compound **Y-*pyr*-EG**.

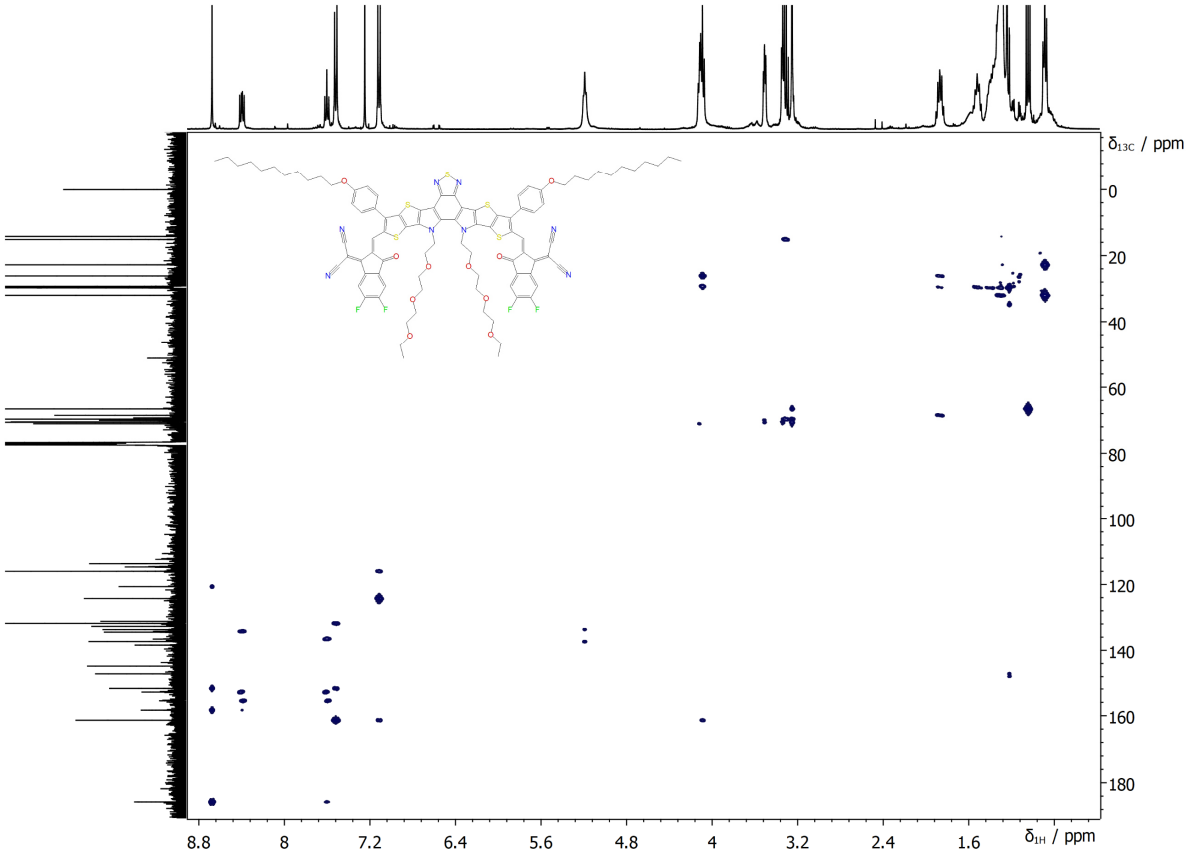

Fig. S43 HMBC NMR (400 MHz) spectrum of compound **Y-*pyr*-EG**.

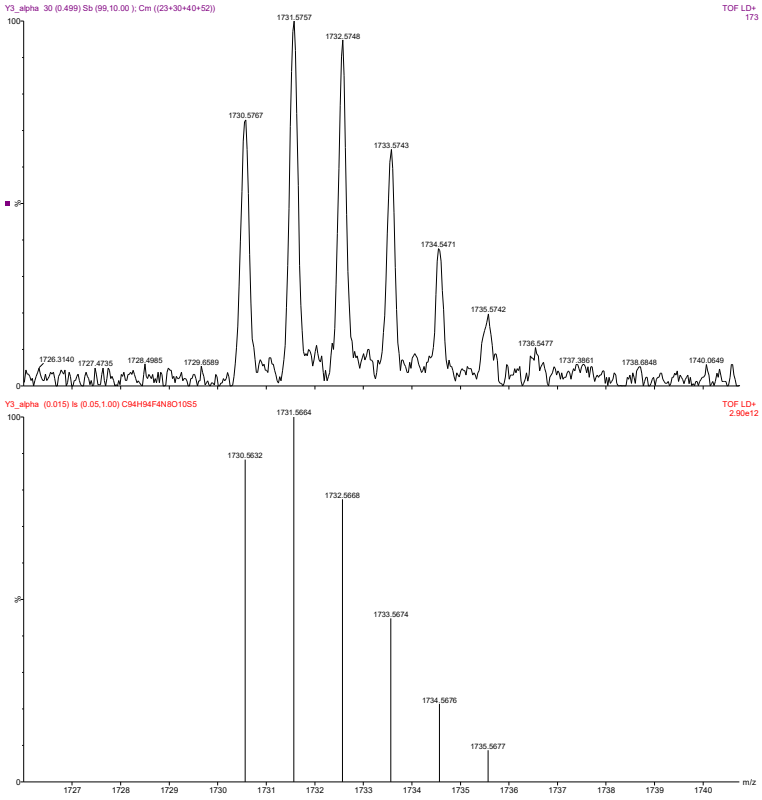

Fig. S44 HR-MS (MALDI-TOF) spectrum (top - measured, bottom - simulated) of compound **Y-*pyr*-EG**.

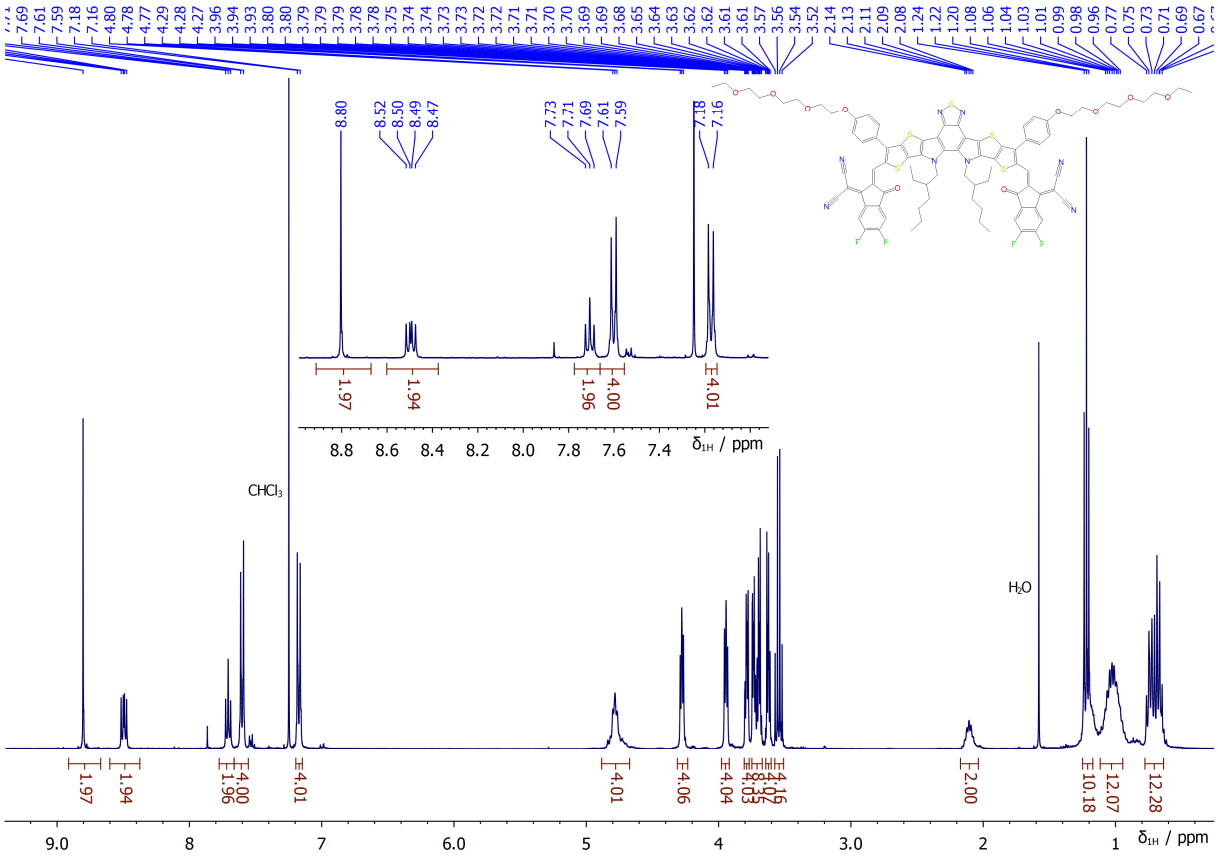

Fig. S45 ^{1}H NMR (400 MHz) spectrum of compound **Y-*thio*-EG**.

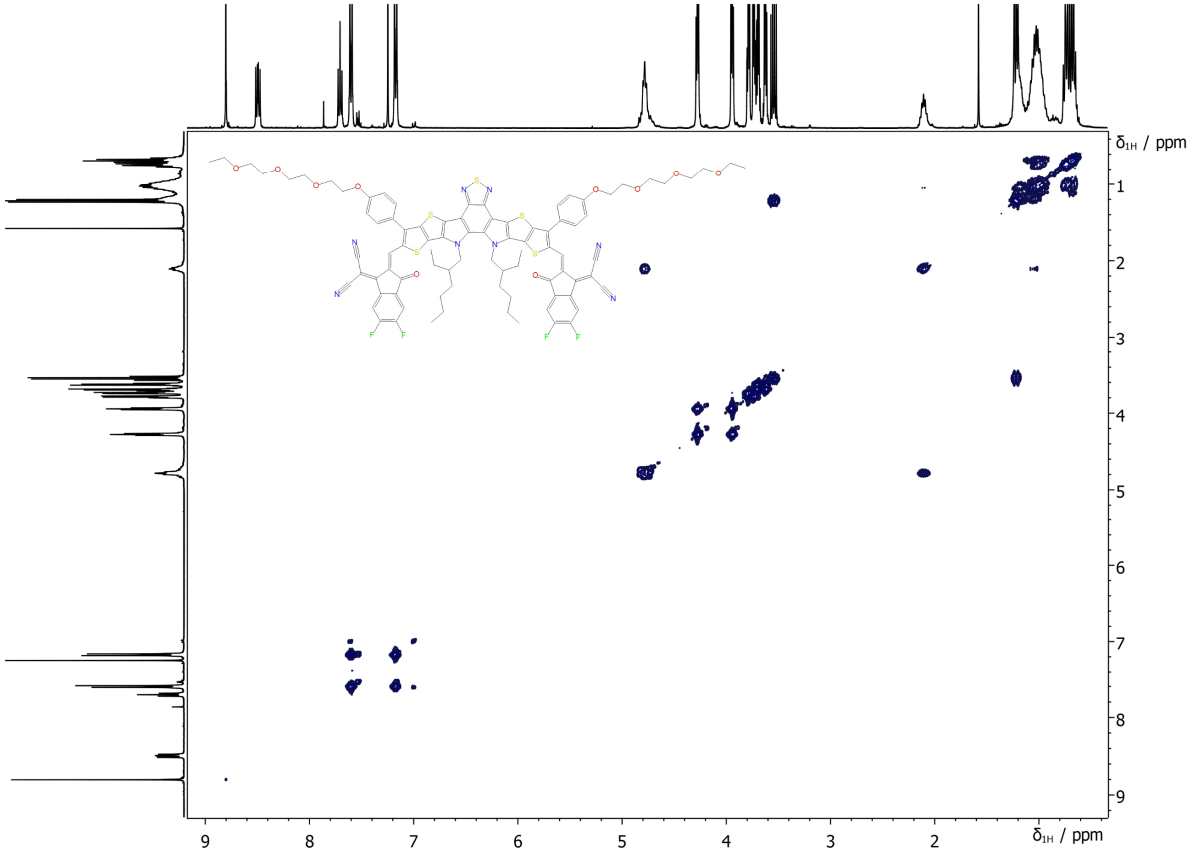

Fig. S46 COSY NMR (400 MHz) spectrum of compound **Y-*thio*-EG**.

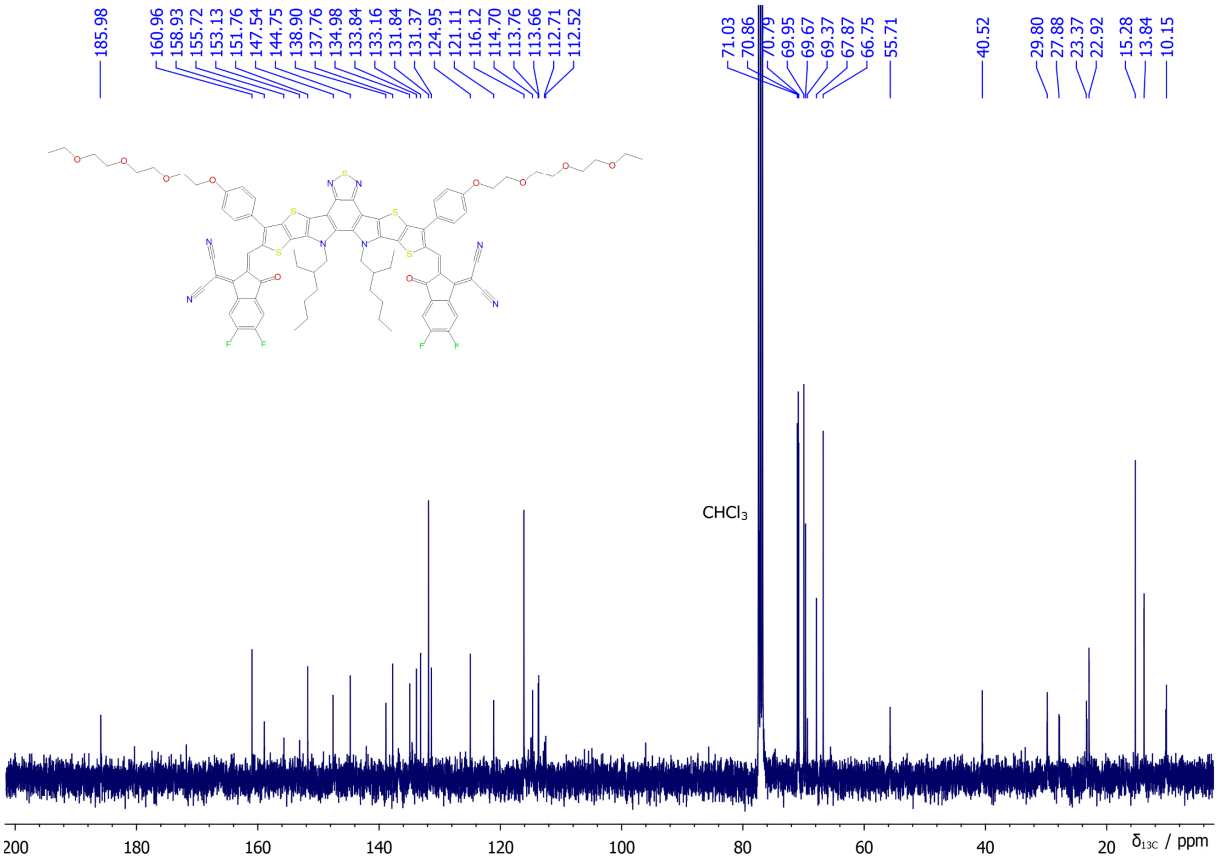

Fig. S47 ^{13}C NMR (100 MHz) spectrum of compound **Y-*thio*-EG**.

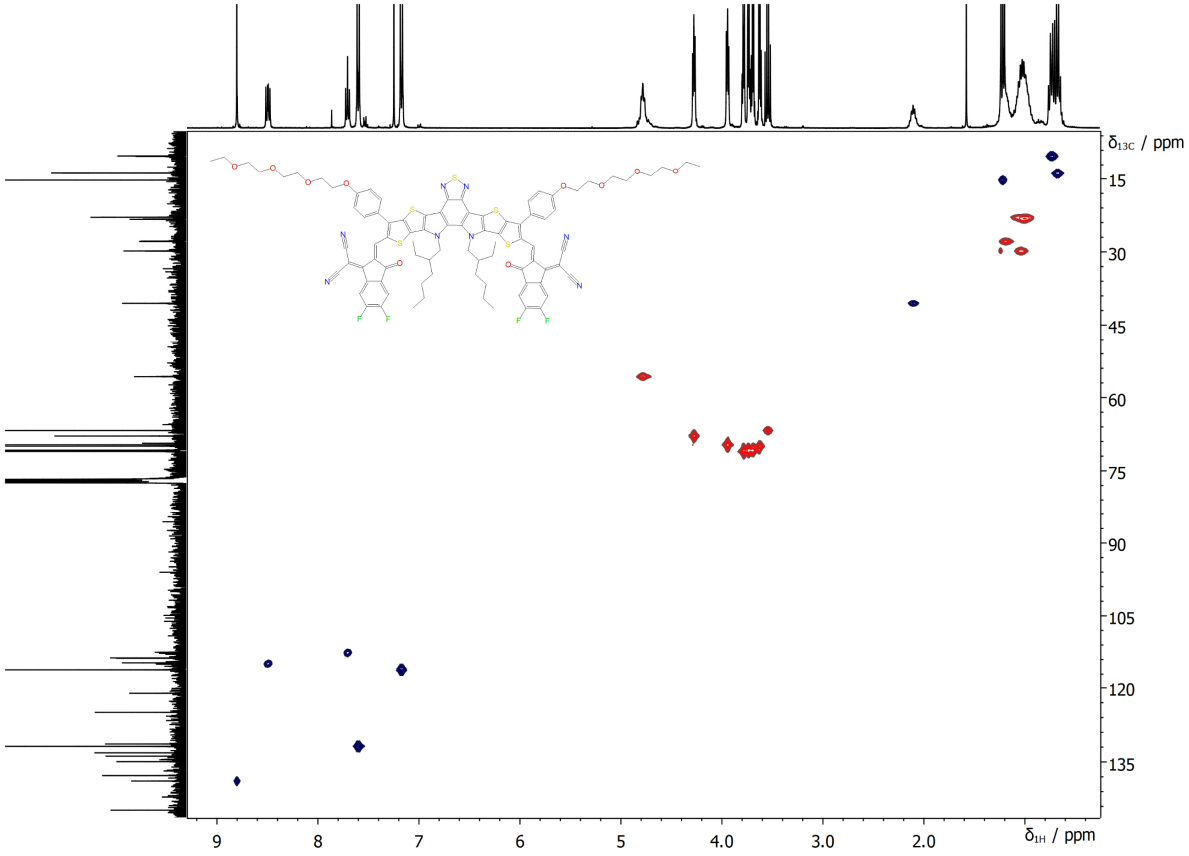

Fig. S48 HSQC NMR (400 MHz) spectrum of compound **Y-*thio*-EG**.

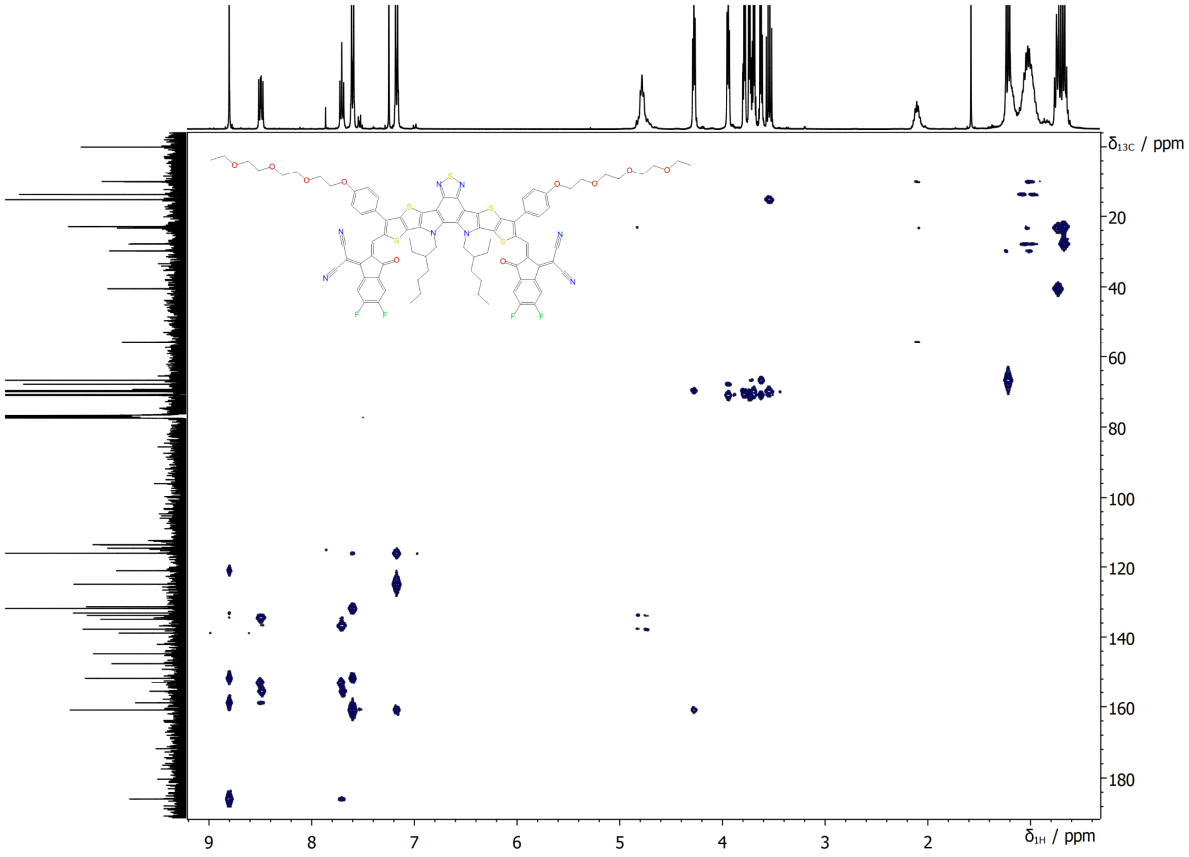

Fig. S49 HMBC NMR (400 MHz) spectrum of compound **Y-*thio*-EG**.

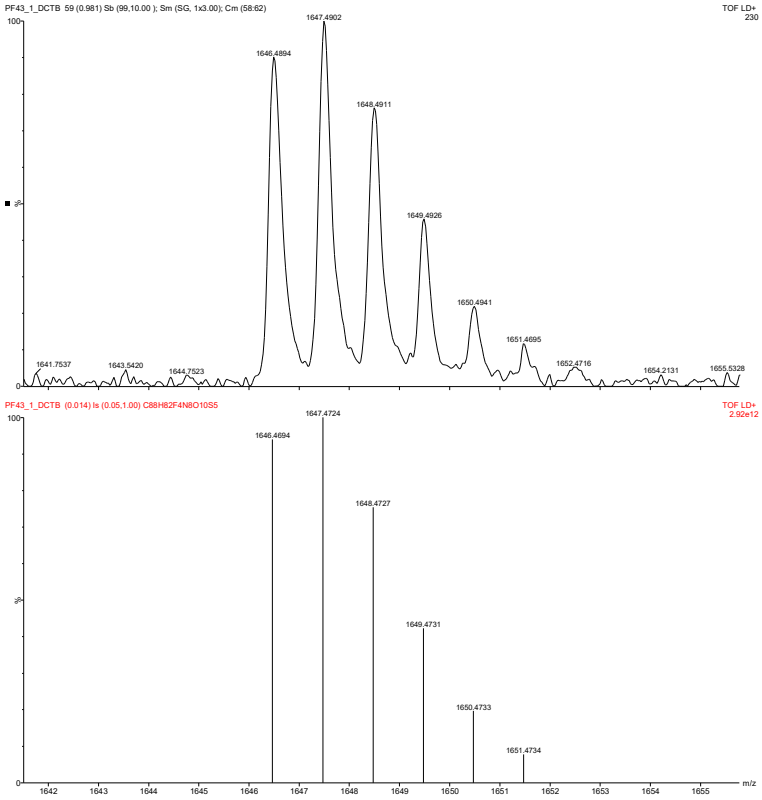

Fig. S50 HR-MS (MALDI-TOF) spectrum (top - measured, bottom - simulated) of compound **Y-*thio*-EG**.

References

1 C. M. Cardona, W. Li, A. E. Kaifer, D. Stockdale and G. C. Bazan, *Adv. Mater.*, 2011, **23**, 2367–2371.

2 T. Nishinaga, *Organic redox systems. Synthesis, properties, and applications*, Wiley, Hoboken, New Jersey, 2016.

3 C. Grazioli, C. Callegari, A. Ciavardini, M. Coreno, F. Frassetto, D. Gauthier, D. Golob, R. Ivanov, A. Kivimäki, B. Mahieu, B. Bučar, M. Merhar, P. Miotti, L. Poletto, E. Polo, B. Ressel, C. Spezzani and G. de Ninno, *Rev. Sci. Instrum.*, 2014, **85**, 23104.

4 G. N. Derry, M. E. Kern and E. H. Worth, *J. Vac. Sci. Technol. A*, 2015, **33**, 60801.

5 D. K. Owens and R. C. Wendt, *J. Appl. Polym. Sci.*, 1969, **13**, 1741–1747.

6 S. Wu, *J. Polym. Sci., C Polym. Symp.*, 1971, **34**, 19–30.

7 M. Wu, C. Harreiß, C. Ophus, M. Johnson, R. H. Fink and E. Spiecker, *Nat. Commun.*, 2022, **13**, 2911.

8 J. Hofinger, S. Weber, F. Mayr, A. Jodlbauer, M. Reinfelds, T. Rath, G. Trimmel and M. C. Scharber, *J. Mater. Chem. A*, 2022, **10**, 2888–2906.

9 E. Wang, L. Hou, Z. Wang, S. Hellström, W. Mammo, F. Zhang, O. Inganäs and M. R. Andersson, *Org. Lett.*, 2010, **12**, 4470–4473.

10 T. Celiker, R. İsci, K. Kaya, T. Ozturk and Y. Yagci, *J. Polym. Sci.*, 2020, **58**, 2327–2334.

11 S. Oh, A. Nikolaev, K. Tagami, T. Tran, D. Lee, S. Mukherjee, R. A. Segalman, S. Han, J. Read de Alaniz and M. L. Chabinyc, *ACS Appl. Mater. Interfaces*, 2021, **13**, 5319–5326.

12 P. Fürk, J. Hofinger, M. Reinfelds, T. Rath, H. Amenitsch, M. C. Scharber and G. Trimmel, *Monatsh. Chem.*, 2022. DOI: 10.1007/s00706-022-02956-2.

13 P. K. Sharma, M. He, L. J. Romanczyk and H. Schroeter, *J. Label Compd. Radiopharm.*, 2010, **53**, 605–612.
14 G. Chai, Y. Chang, J. Zhang, X. Xu, L. Yu, X. Zou, X. Li, Y. Chen, S. Luo, B. Liu, F. Bai, Z. Luo, H. Yu, J. Liang, T. Liu, K. S. Wong, H. Zhou, Q. Peng and H. Yan, *Energy Environ. Sci.*, 2021, **14**, 3469–3479.